

WKB Method and Quantum Periods beyond Genus One

Fabian Fischbach¹, Albrecht Klemm², Christoph Nega³

¹²³*Bethe Center for Theoretical Physics and ²Hausdorff Center for Mathematics,
Universität Bonn, D-53115 Bonn*

Abstract

We extend topological string methods in order to perform WKB approximations for quantum mechanical problems with higher order potentials efficiently. This requires techniques for the evaluation of the relevant quantum periods for Riemann surfaces beyond genus one. The basis of these quantum periods is fixed using the leading behaviour of the classical periods. The full expansion of the quantum periods is obtained using a system of Picard-Fuchs like operators for a sequence of integrals of meromorphic forms of the second kind. Discrete automorphisms of simple higher order potentials allow to view the corresponding higher genus curves as covering of a genus one curve. In this case the quantum periods can be alternatively obtained using the holomorphic anomaly solved in the holomorphic limit within the ring of quasi modular forms of a congruent subgroup of $SL(2, \mathbb{Z})$ as we check for a symmetric sextic potential.

¹fischbach@physik.uni-bonn.de

²aklemm@th.physik.uni-bonn.de

³cnega@th.physik.uni-bonn.de

1 Introduction and Summary

Periods of differentials of first, second and third kind on Riemann surfaces Σ_g with genus $g \geq 1$ are a classical mathematical subject generalizing the theory of elliptic functions. These periods have rich applications to N=2 super symmetric gauge theory [1, 2], topological string theory on local Calabi-Yau manifolds [3, 4], matrix models [5] and integrable models [6, 7]. Additional connections to Liouville Theory and more general 2d CFTs have been proposed in [8] and at a more technical level the periods are related to certain Feynman integrals [9].

The supersymmetric gauge theories exhibit a two parameter ϵ_1, ϵ_2 space of deformations, the so called Ω -background, that allows to solve it by localization [10], while the topological string has generically only a world-sheet genus g_{ws} expansion in the string coupling g_s corresponding to $g_s^2 = \epsilon_1 \epsilon_2$. However, in the presence of global $U(1)_R$ symmetry on the geometry it can be uniquely refined motivically to exhibit two deformation parameters say g_s and $s = (\epsilon_1 + \epsilon_2)^2$ [11]. The matrix model has a genus expansion and also a candidate for refinement of the measure [12], while the particular integrable structure [6] occurs in the Nekrasov-Shatashvili limit⁴ $\epsilon_2 = 0$. The connections between these theories are mostly well understood. The N=2 super symmetric gauge theory is related to the topological string by the geometric engineering limit [2]. The relation between the topological string and the matrix models was made precise in [13].

It has been pointed out in [7] that the genus expansion of the topological string can be viewed as a time dependent quantization of the geometry of the Riemann surface and in [14] it has been recognized that the \hbar expansion in the Nekrasov-Shatashvili limit (NS limit) can be literally viewed as a time independent WKB quantisation of an action given by the classical periods, which encode the potential of the quantum mechanical problem. This yields as solution to the WKB problem the \hbar expansion of the quantum periods. More concretely it has been exemplified in [15] that solving the holomorphic anomaly equation can be turned into an efficient formalism to obtain these quantum periods of simple WKB problems. This seems independent of the fact whether Σ_g corresponds topological string-, gauge theory- or a matrix model spectral curve. Quantum mechanical problems that do correspond to a gauge theory curve have been considered in [16]. In particular near the Argyres-Douglas points for $SU(2)$ with one and two flavors in the fundamental representation, the families of Seiberg-Witten curves describing the deformation away from the conformal point can be mapped exactly to the quantum mechanical problems with cubic and the quartic potential [16]. As a consequence the quantized curve describes the gauge theory coupled to an Ω -background. A similar analysis could be done for the Argyres-Douglas points in the Coulomb branch of higher rank gauge groups.

The holomorphic anomaly equations originate in the worldsheet B-model approach to topological string theory [17] which has only a g_s expansion. For the present purpose they have to be refined as in [18, 19]. The resulting equations are recursively

⁴We will denote the remaining deformation $\epsilon_1 = \hbar$.

based as starting data on the holomorphic genus zero free energy $F_0 = F^{(0,0)}(t)$, which can be interpreted as the classical term, the an-holomorphic genus one free energy $F^{(0,1)}(t)$, whose an-holomorphicity is given by a second order $\partial_t \bar{\partial}_t$ differential equation for the Ray-Singer torsion [17] giving g_s^2 corrections and a meromorphic function $F_1 = F^{(1,0)}(t)$, which is proportional to the logarithm of the discriminant of Σ_g and gives \hbar^2 corrections. More generally the holomorphic anomaly equation for each $F^{(m,n)}(t)$ with $(m+n) \geq 2$ has a *recursion kernel* called the holomorphic ambiguity, whose *finite dimension* has a polynomial growth in (n, m) . It has been argued in [20] that for gauge theory and matrix models this holomorphic ambiguity can be fixed by the gap condition at the conifold divisors and regularity at the orbifold divisors in the moduli space. In [21] it has been shown that this is more generally true for the genus expansion of the topological string on local geometries whose mirrors are genus g curves. These arguments have been extended to the refined theories whose B-model description are genus g curves. For this class the set of sufficient boundary conditions has been specified in [18, 22]. They imply, of course, the integrability of the theory in the NS limit, in which it is considerably simpler.

In particular, one can obtain in these cases the quantum periods by solving the holomorphic anomaly equation [23]. Alternatively, one can consider the quantum expansion of the differential in \hbar^2 , which is apart from the leading term in \hbar always of the second kind and solve the quantum period using a system of Picard-Fuchs like differential operators \mathcal{D}_{2n} that yield the \hbar^{2n} correction term from the classical period as proposed in [24].

In this paper we extend both methods to higher genus curves. As it turns out the formalism using the holomorphic anomaly equation is slightly more convenient in the $g = 1$ case, because one can use very efficiently the modularity properties of genus one curves as developed in [22]. One needs essentially only the genus one curve in the Weierstrass form, the transformation into which is easily done using Nagell's algorithm. This method solves right away all cases with quantum mechanical problems whose potential is of quartic or cubic degree. However, we find that some symmetric higher degree quantum mechanical potentials describe higher genus curves which are multi-coverings of genus one curves. In this case the higher genus problem can be reduced to a genus one problem and solved as such very efficiently as described above. In particular, we check along these lines that the gap condition appropriately determines the right boundaries of the WKB problem with a sextic curve covering a quartic curve. Higher degree potentials are of course particularly interesting if this symmetry can be broken at will by arbitrary perturbations which leads to really independent cycles or branch cuts which can capture interesting changes in the possible non-perturbative effects.

Despite the fact that part of the original motivation of this work was to use the extension of the $\text{SL}(2, \mathbb{Z})$ modular approach of the $g = 1$ case to the one of Siegel modular forms in the higher genus case in order to solve the holomorphic anomaly equation as in [25], it has turned out to be much easier to extend the \mathcal{D}_{2n} to a system of multi-parameter operators that yield the higher \hbar correction terms from the classical periods. We develop this formalism, which applies to arbitrary genus, and exemplify

it with the quintic potential with additional deformation parameters turned on. Our ability to solve quantum periods on higher genus curves for arbitrary multi-parameter complex deformation families will also shed light on the problem of how to restrict the general parametrization of higher genus curves by the Siegel upper half plane to those algebraic deformations of the potential that occur in a specific quantum mechanical setting, which we leave, however, for future explorations. Quantum periods could lead to a generalization of the semiclassical analysis of 1D multivalent Coulomb gases mapped to (non-)Hermitian quantum mechanics [26], where the classical periods of families of Riemann surfaces of genus $g \geq 1$ yield information about the energy spectrum and bandwidth (i.e. pressure and transport barrier).

Note: While we were preparing this preprint, the paper [27] appeared, which has overlap in determining the quantum periods by the Picard-Fuchs differential systems, but only in the modular cases related to genus one curves, where the method was already discussed in [24] and the direct integration method is more efficient.

2 The All-Orders WKB Method

2.1 The WKB Ansatz

This section provides a quick introduction to the all-orders WKB method of Dunham [28]⁵. A central object in this method is the *quantum period*, a formal power series in \hbar^2 whose $\hbar \rightarrow 0$ limit yields a phase space volume defined by a maximal energy ξ . Let us explain the construction. Consider the one-dimensional Schrödinger equation for a particle moving in a potential V ,

$$\hbar^2 \psi''(x) + p^2(x) \psi(x) = 0, \quad p(x) = \sqrt{2(\xi - V(x))}, \quad (2.1)$$

where the mass has been set to $m = 1$. The WKB ansatz for the wavefunction

$$\psi(x) = \exp \left[\frac{i}{\hbar} \int^x Q(x') dx' \right] \quad (2.2)$$

turns the Schrödinger equation into a Riccati equation for $Q(x)$,

$$Q^2(x) - i\hbar \frac{dQ(x)}{dx} = p^2(x), \quad (2.3)$$

which in turn is expanded in a formal power series

$$Q(x) = \sum_{n=0}^{\infty} Q_n(x) \hbar^n \quad (2.4)$$

and leads to a recursion for the functions $Q_n(x)$,

$$Q_0(x) = p(x) \\ Q_{n+1}(x) = \frac{1}{2Q_0(x)} \left(i \frac{\partial}{\partial x} Q_n(x) - \sum_{k=1}^n Q_k(x) Q_{n+1-k}(x) \right). \quad (2.5)$$

⁵Our exposition closely follows [15]. For a more pedagogical treatment we refer to [29].

Splitting the series into even and odd powers of \hbar ,

$$Q(x) = Q_{\text{odd}}(x) + P(x), \quad P(x) = \sum_{n=0} Q_{2n}(x) \hbar^{2n}, \quad (2.6)$$

one finds that $Q_{\text{odd}}(x)$ is a total derivative

$$Q_{\text{odd}}(x) = \frac{i\hbar}{2} \frac{P'(x)}{P(x)} = \frac{i\hbar}{2} \log P(x) \quad (2.7)$$

and it follows that only Q_1 and P contribute to period integrals of (2.4). The WKB wavefunction (2.2) can be rewritten in terms of $P(x)$ only, i.e.,

$$\psi(x) = \frac{1}{\sqrt{P(x)}} \exp \left[\frac{i}{\hbar} \int^x P(x') dx' \right]. \quad (2.8)$$

Now consider the family of (compact) Riemann surfaces Σ defined by

$$\Sigma : \quad y^2 = p^2(x), \quad (2.9)$$

where the energy ξ and possibly parameters of the potential V serve as family parameters. In the following we restrict ourselves to polynomial potentials such that Σ becomes a family of hyperelliptic curves. The genus $g = \lfloor \frac{d-1}{2} \rfloor$ is then determined by the degree d of the potential.

For anharmonic oscillators leading to a genus one curve there are only two independent one-cycles on the curve, one of which typically encircles the branch points bounding a classically allowed region. We call it the A -cycle. On the other hand, the B -cycle corresponds to a classically forbidden region. The volume of the classically allowed region in phase space can be expressed as the period integral of the one-form $y(x) dx$ as

$$\frac{1}{\pi} \text{vol}_0(\xi) = \frac{1}{2\pi} \oint_A y(x) dx. \quad (2.10)$$

Its quantum counterpart is then defined using the formal series for $P(x) dx$,

$$\nu = \frac{1}{2\pi} \oint_A P(x) dx, \quad (2.11)$$

and appears in the all-orders WKB quantization condition

$$\nu = \hbar \left(n + \frac{1}{2} \right), \quad n = 0, 1, 2, \dots \quad (2.12)$$

The questions of how to generalize this quantization condition to (1.) several potential wells separated by barriers (as it is generic for higher genus curves) and to (2.) include non-perturbative effects shall not be addressed here. Indeed, we will only be interested in providing efficient computational methods for WKB quantum periods and in probing the conjectural connection between these periods and the holomorphic anomaly equation.

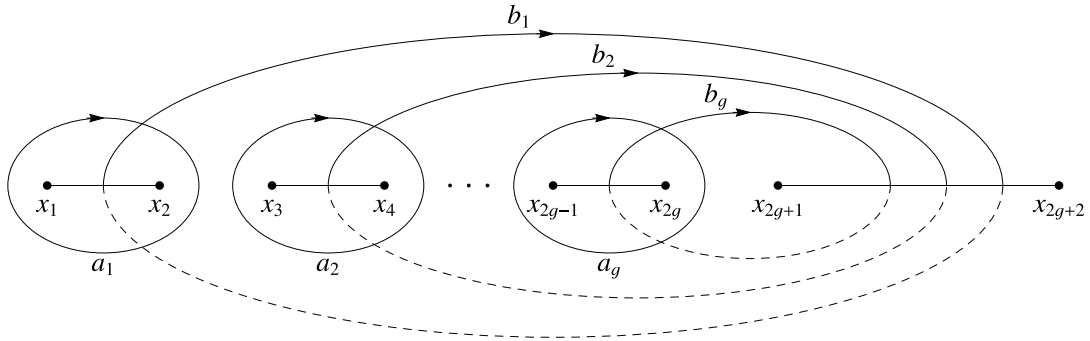


Figure 2.1: A canonical basis of one-cycles for a hyperelliptic curve. Branch points x_j are algebraic functions of ξ . Dotted path segments lie on the other sheet.

2.2 Geometry of Quantum Periods

In the following we collect some facts⁶ about the geometry and topology of hyperelliptic curves, tailored to the WKB setup and yielding explicit constructions.

Moduli Space of Hyperelliptic Curves. A compact Riemann surface of genus $g \geq 2$ has $\dim_{\mathbb{C}} \mathcal{M}_g = 3g - 3$ moduli, while the moduli space of hyperelliptic curves is of dimension $\dim_{\mathbb{C}} \mathcal{M}_g^{\text{hyp}} = 2g - 1$. To understand the latter, note that the branch points serve as local parameters of $\mathcal{M}_g^{\text{hyp}}$. Two hyperelliptic (or elliptic) curves are conformally equivalent if and only if their branch points differ by a fractional linear transformation (Möbius transformation)

$$x \mapsto \frac{\alpha x + \beta}{\gamma x + \delta}, \quad \begin{pmatrix} \alpha & \beta \\ \gamma & \delta \end{pmatrix} \in \text{PSL}(2, \mathbb{C}). \quad (2.13)$$

These are precisely the bijective holomorphic maps $\hat{\mathbb{C}} \rightarrow \hat{\mathbb{C}}$. Hence $\dim_{\mathbb{C}} \mathcal{M}_g^{\text{hyp}} = (2g + 2) - \dim_{\mathbb{C}} \text{PSL}(2, \mathbb{C}) = 2g - 1$ as claimed.

From the WKB point of view the energy ξ is a natural curve parameter and a choice of the potential V selects a sublice of $\mathcal{M}_g^{\text{hyp}}$.

Degenerations and Monodromies. For a polynomial $V(x)$ the complex curve Σ can be regarded as two copies of the Riemann sphere $\hat{\mathbb{C}} = \mathbb{P}^1$, glued together along branch cuts. Here the branch points are turning points of classical trajectories and their complex analogs⁷, given by $p^2(x) = 0$. There are $\dim_{\mathbb{C}} H_1(\Sigma, \mathbb{C}) = 2g$ independent one-cycles on Σ , which can be represented by closed contours encircling branch points. This is schematically shown in Fig. 2.1. For certain values of ξ two (or more) branch points coincide and a corresponding one-cycle vanishes. Pictorially,

⁶The mathematical statements we have collected here are mostly textbook knowledge. A good introduction to Riemann surfaces with application to periods is given in [30].

⁷If $V(x)$ has odd degree, one branch point lies at infinity.

a handle of the surface described by Σ gets pinched and Σ is called degenerate or singular. Indeed, the curve is non-singular if and only if the discriminant

$$\text{discr}_x p^2(x) = c \prod_{i < j} (x_i - x_j)^2 \quad (2.14)$$

is non-zero. This is always a polynomial in the coefficients multiplying the monomials of $p^2(x)$. Generically, there are no radical expressions for the roots x_i if $d > 5$ (Abel-Ruffini), nevertheless the discriminant can be factorized as⁸

$$\Delta(\xi) = \prod_{i=1}^{d-1} (\xi - V(x_i^{(c)})) \quad (2.15)$$

where the $x_i^{(c)}$ are the critical points of $V(x)$. Thus, for fixed potential $V(x)$, eq. (2.9) defines a smooth fiber bundle $\mathcal{S} \xrightarrow{\pi} \mathcal{B}$ over the base $\mathcal{B} = \mathbb{P}^1 \setminus (\{\Delta = 0\} \cup \{\infty\})$, the fibers being smooth hyperelliptic curves. Moreover, the homology groups $H_1(\Sigma, \mathbb{C})$ of the fibers combine to a complex vector bundle over the same base \mathcal{B} . Fixing a reference point ξ in \mathcal{B} for the moment, it can be shown [30] that there is a monodromy homomorphism⁹

$$\rho_{\text{mon.}} : \pi_1(\mathcal{B}, \xi) \rightarrow \text{GL}(H_1(\Sigma_\xi, \mathbb{C})) \quad (2.16)$$

whose image can be identified with a discrete subgroup of $\text{Sp}(2g, \mathbb{Z})$, i.e., it preserves the symplectic structure defined by the intersection form \cap . The image of (2.16) is the *monodromy group* of the family of curves. For the generator g' associated to a point ξ' with vanishing cycle γ' the monodromy action on a cycle $\gamma \in H_1(\Sigma_\xi, \mathbb{C})$ is given by the Picard-Lefschetz formula

$$\rho_{\text{mon.}}(g') : \gamma \mapsto \gamma + (\gamma' \cap \gamma) \gamma'. \quad (2.17)$$

Geometrically this is a Dehn twist along the embedded circle representing γ' . There is a neighborhood N of this circle homeomorphic to a cylinder $[-1, 1] \times \mathbb{S}^1$. If γ is another embedded circle intersecting γ' exactly once with the intersection point lying in N , then Fig. 2.2 shows the action corresponding to (2.17). The upshot is that this monodromy determines the structure of the periods $\Pi(\xi)$ on Σ , which are sections of the same vector bundle over \mathcal{B} (up to isomorphism). This will become explicit when discussing Picard-Fuchs equations shortly.

Abelian Differentials. The WKB periods belong to a tower of meromorphic one-forms $\mathcal{Q}_n = Q_n(x) dx$ on Σ . Meromorphic one-forms on Riemann surfaces are usually divided into three types: *Abelian differentials of the first kind* are holomorphic, i.e., in any local complex coordinate (z, U) they can be written as $\lambda = \lambda_z dz$ with a

⁸This can be seen as follows: up to a constant the discriminant is the resultant of $(\xi - V(x))$ and $V'(x)$, which vanishes if and only if the two possess a common root.

⁹The fundamental group of the base appearing here is generated by loops starting at ξ and encircling single points of $\{\Delta = 0\} \cup \{\infty\}$ in some fixed direction once (see Fig. 4.1b for an example).

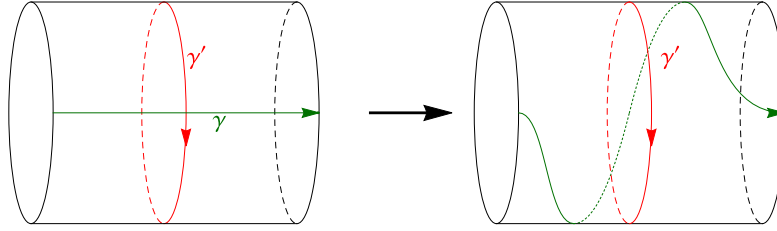


Figure 2.2: Dehn twist along an embedded circle γ' .

holomorphic function λ_z . For hyperelliptic curves of genus g there are precisely g such forms modulo exact forms, a basis is given by the g differentials $x^j dx/y$, $j = 0, \dots, g-1$. There are also *Abelian differentials of the second kind* where λ_z is a meromorphic function with vanishing residues. They form an infinite-dimensional vector space $\Lambda^1(\Sigma)$. An *Abelian differential of the third kind* is also allowed to have non-zero residues in its local Laurent expansion.

It is well known that the middle cohomology $H^1(\Sigma, \mathbb{C})$ has complex dimension $2g$ and can be represented as the quotient

$$H^1(\Sigma, \mathbb{C}) = \frac{\Lambda^1(\Sigma)}{\text{Im}(d : \Lambda^0(\Sigma) \rightarrow \Lambda^1(\Sigma))}, \quad (2.18)$$

where d denotes the exterior derivative and we have introduced $\Lambda^0(\Sigma) = \{\phi : \Sigma \rightarrow \mathbb{P}^1 \mid \phi \text{ meromorphic}\}$. Clearly non-zero residues obstruct homotopy invariance, which is required for a well-defined pairing between singular homology $H_1(\Sigma, \mathbb{C})$ and cohomology $H^1(\Sigma, \mathbb{C})$. Some computation will be required to see which WKB differentials are of third or second kind.

Picard-Fuchs Equations. Periods of differentials of the second kind satisfy ordinary differential equations with respect to the modulus ξ , which are at most of order $2g$. To see this, recall that any period and its derivatives produce local sections of a vector bundle over \mathcal{B} , the fibers being isomorphic to $H^1(\Sigma, \mathbb{C})$. Finite dimensionality then requires a linear relation amongst the derivatives. These *Picard-Fuchs equations* (PFE) are of Fuchsian type and fundamental systems can be constructed by Frobenius' method [31].

To find the PFE for the WKB periods at each order in \hbar^2 we use the identification (2.18) and start by considering the WKB differentials. For each $n \in \{0, 1, 2, \dots\}$ there is a polynomial p_n in x and ξ of degree

$$\deg_x p_n \leq n(d-1) \quad (2.19)$$

in x such that

$$Q_n = \frac{p_n}{y^{3n-1}}. \quad (2.20)$$

Polynomials for $n \geq 2$ satisfy the recursion relation

$$p_{n+1} = \frac{i}{2} (2p'_n (\xi - V) + (3n - 1)p_n V') - \frac{1}{2} \sum_{k=1}^n p_k p_{n+1-k}, \quad p_0 = 1, \quad p_1 = \frac{-i}{2} V' \quad (2.21)$$

where $(\dots)'$ means $\partial_x(\dots)$. As V is a real polynomial, p_{2n} (p_{2n+1}) has real (imaginary) coefficients. Linear dependence in $H^1(\Sigma, \mathbb{C})$ hence translates into the ansatz

$$\sum_{i=0}^r f_i(\xi) \frac{\partial^i}{\partial \xi^i} \left(\frac{p_n}{y^{3n-1}} \right) - \sum_{k=0}^{k_{\max}} \frac{\partial}{\partial x} \left(\alpha_k(\xi) \frac{x^k}{y^{3n-3+2r}} \right) = 0 \quad (2.22)$$

for some $r \leq 2g$ and sufficiently large k_{\max} . After writing the expression with $y^{3n-1+2r}$ as common denominator, we choose the α_k to subsequently eliminate monomials $g_j(\xi)x^j$ from the resulting numerator, starting from the highest power in x . Some monomials will remain and requiring their coefficients to vanish determines the polynomials $f_i(\xi) \in \mathbb{Z}[\xi]$ up to an overall constant. Thus, we find the PFE

$$\sum_{i=0}^r f_i(\xi) \frac{\partial^i \Pi(\xi)}{\partial \xi^i} = 0 \quad \text{for} \quad \Pi(\xi) = \oint_{\gamma} Q_n \, dx. \quad (2.23)$$

The polynomial in front of the highest derivative is actually the discriminant Δ encountered before, i.e., degenerations of Σ are in one-to-one-correspondence with the regular singular points of the PFE. The relation to Picard-Lefschetz theory becomes even clearer when regarding the analytic structure of solutions to the PFE (2.23): the series ansatz

$$\Pi(\xi) = \xi^r \sum_{k=0}^{\infty} c_k \xi^k \quad (2.24)$$

leads to a polynomial *indicial equation* for r^{10} . Here we seek solutions around $\xi = 0$. After having solved for r a recursion relation for the coefficients $c_k^{(r)}$ of each r -solution is to be found. If the roots of the indicial polynomial are pairwise distinct and no two of them differ by an integer, this construction already leads to a fundamental system. In case two roots differ by an integer, without loss of generality $r_1 - r_2 \in \{0, 1, 2, \dots\}$ and Π_{r_1} is a solution of the form (2.24), a linearly independent solution may be found using the ansatz

$$\Pi_{r_2}(\xi) = c \cdot \Pi_{r_1}(\xi) \log(\xi) + \sum_{k=0}^{\infty} d_k \xi^{k+r_2} \quad (2.25)$$

where the constant c might be zero if $r_1 - r_2 \neq 0^{11}$. Consider the special case of a double indicial root $r_1 = r_2 = 1$, so the analytic solution $\Pi_1(\xi) = \xi + \dots$ vanishes as $\xi \rightarrow 0$. The second solution $\Pi_{1'}$ for the given index $r = 1$ takes the form (2.25)

¹⁰The exponent r appearing in this ansatz is not to be confused with the order r of the Picard-Fuchs equation (2.23).

¹¹For a more complete discussion of Frobenius' method the reader may wish to consult [32] or [31].

with $c \neq 0$, without loss of generality $c = (2\pi i)^{-1}$, and thus possesses the monodromy property encountered in the Picard-Lefschetz formula: analytic continuation along a closed path enclosing $\xi = 0$ shifts $\Pi_{1'} \rightarrow \Pi_{1'} + \Pi_1$ due to the logarithm. This monodromy property allows us to identify Π_1 with the period integral of the respective one-form along a one-cycle that vanishes as $\xi \rightarrow 0$ (up to normalization). Also, $\Pi_{1'}$ belongs to periods along cycles non-trivially intersecting with the vanishing cycle.

Differential Operators for Quantum Corrections. Exploiting linear dependence modulo exact forms we also obtain differential operators $\hbar^{2n}\mathcal{D}_{2n}$ that generate quantum corrections when acting on classical WKB periods $\oint Q_0 dx$. Derivatives of the latter span a subspace of $H^1(\Sigma, \mathbb{C})$, in all examples considered the full space, so an ansatz analogous to eq. (2.22) is justified. In the above fashion we find rational functions $q_i^{(2n)}(\xi) \in \mathbb{Q}(\xi)$ such that

$$\mathcal{D}_{2n}Q_0 := \left[\sum_{i=0}^{2g-1} q_i^{(2n)}(\xi) \frac{\partial^i}{\partial \xi^i} \right] Q_0 = Q_{2n} + \partial_x(\dots). \quad (2.26)$$

We stress that these results provide an efficient method of computing WKB periods up to arbitrary order in \hbar^2 . First one computes the classical PFE and uses Frobenius' method to provide a fundamental system of solutions. The difficult point is to compute a few terms¹² of the classical hyperelliptic periods $\oint y dx$ in order to fix the corresponding linear combination of solutions. Applying $\hbar^{2n}\mathcal{D}_{2n}$ on those bypasses further evaluation of period integrals.

3 Holomorphic Anomaly Equation and Direct Integration

3.1 Connecting WKB to the Holomorphic Anomaly Equation

Having introduced the WKB method and discussed the geometry behind its periods we are now able to connect the latter to the holomorphic anomaly equation governing refined topological string free energies. Guided by [15] we take from the WKB recursion (2.5) the formal power series

$$P(x) = \sum_{n=0}^{\infty} Q_{2n}(x) \hbar^{2n}. \quad (3.1)$$

In the examples discussed in [15] there is a canonical symplectic pair (A, B) of cycles, called the perturbative and non-perturbative cycle, encircling pairs of branch points

¹²In appendix B we show how to compute the leading behaviour of the classical periods by means of an example.

localized on the real axis. With these cycles we define the quantum A - and B -period

$$\nu(\xi) = \sum_{n=0}^{\infty} \nu^{(2n)} \hbar^{2n} = \frac{1}{2\pi} \sum_{n=0}^{\infty} \hbar^{2n} \oint_A Q_{2n} dx \quad (3.2)$$

$$\nu_D(\xi) = \sum_{n=0}^{\infty} \nu_D^{(2n)} \hbar^{2n} = -i \sum_{n=0}^{\infty} \hbar^{2n} \oint_B Q_{2n}(x) dx . \quad (3.3)$$

We call the inverse of the A -period (3.2) the quantum mirror map¹³

$$\xi(\nu) = \sum_{n=0}^{\infty} \xi_n(\nu) \hbar^{2n} . \quad (3.4)$$

Then the quantum free energy is defined by

$$\frac{\partial F}{\partial \nu} = \nu_D \quad (3.5)$$

which makes it obvious that the quantum free energy admits an \hbar expansion

$$F(\nu) = \sum_{n=0}^{\infty} F_n(\nu) \hbar^{2n} . \quad (3.6)$$

As $F(\nu)$ was defined via its ν -derivative it is not possible to fix the constant term of the free energy from the WKB perspective¹⁴.

Inspired by this construction Codesido and Marino [15] claimed that free energies (3.5) corresponding to all-orders WKB periods (3.2) and (3.3) of generic one-dimensional quantum systems are governed by the refined holomorphic anomaly equation characterizing the refined topological string free energies in the Nekrasov-Shatashvili limit.

3.2 Sub-slices in the Moduli Space of Hyperelliptic Curves

On a genus g Riemann surface Σ_g it is always possible to choose a symplectic basis (A_i, B^i) , $i = 1, \dots, g$, of the homology $H_1(\Sigma_g, \mathbb{Z})$ with $A_i \cap B^j = \delta_i^j$ and accordingly one has in general several A -periods $\nu_i(\xi, \eta)$ and several B -periods $\nu_{D_i}(\xi, \eta)$ respectively. Moreover, on a hyperelliptic curve Σ_g they can in the general case depend, besides of the energy ξ corresponding to the constant term in x , on $2g - 2$ perturbations η of the potential.

Easy quantum mechanical potentials correspond to sub-slices in the full moduli space where the branch points of one cut are real. In the simplest cases the periods on this sub-slice enjoy a simple relation due to additional symmetries on Σ_g . For example

¹³The leading term, the *classical* mirror map $\xi_0(\nu)$, is the inverse function of the classical A -period.

¹⁴The authors of [15] however discuss a preferred choice of the constant term, which allows them to write down an integrated form of what is called a PNP-relation for the quantum mirror map specific to the respective systems investigated there.

for a sextic potential that we consider in Section 4.1 two symmetric B cycles are exchanged by \mathbb{Z}_2 symmetry and the problem reduces to one pair of symplectic periods on a genus one curve on which a solution of the holomorphic anomaly, described in some generality in Section 3.3-3.5, can be constructed and perfectly reproduces the quantum period, just using the standard boundary conditions to fix the recursion kernels, as summarised for the particular example in Section 4.1.3. More conceptually one can state that in this case if one can find a subgroup $\Gamma_{\Sigma_1} \subset \mathrm{SL}(2, \mathbb{Z})$ with $\Gamma_{\Sigma_1} \subset \Gamma_{\Sigma_g} \subset \mathrm{Sp}(4, \mathbb{Z})$ on the sub-slice and the generators of almost modular forms of Γ_{Σ_1} can be used to perform the direct integration.

The situation is more complicated if one considers a sub-slice on a higher genus surface when the reality condition of the branch points of one cut is not related to a symmetry, as for example for the particular quintic potential discussed in section 4.2. In this case it is not possible to obtain the solution of the holomorphic anomaly equation by the direct integration directly on the sub-slice. The reason is that the reality condition breaks in general the modular invariance of the $F^{(n,g)}$ under the subgroup $\Gamma_{\Sigma_g} \subset \mathrm{Sp}(2g, \mathbb{Z})$ of the family Σ_g in a very complicated way¹⁵. A modular family is however necessary to write the $F^{(n,g)}$ as polynomials in the ring of modular generators for Γ_{Σ_g} and to perform the direct integration with respect to the almost holomorphic generators. Also in order to determine all boundary data by the gap condition one has to consider in general all possible conifold divisors and some of those might not be accessible in the restricted parametrization of the sub-slice. At the technical level we argue in Section 4.2.3 that on the sub-slice of the quintic one does not find the start datum F_1 that allows to setup the direct integration on the slice directly.

These problems have a conceptually easy, but technically demanding solution: one has to set up the problem first in the full moduli space of the hyperelliptic curve, as it has been done e.g. for $g = 2$ in [25], and then restrict to the sub-slice.

Before setting up the formalism to solve the multi-parameter holomorphic anomaly equation we should mention that we develop a formalism to get the quantum period on the sub-slice and the full moduli space by deriving a system of differential operators \mathcal{D}_{2n} that allow to obtain all quantum periods if the classical periods over a symplectic basis are determined. We demonstrate this for the quintic in section 4.2.

3.3 The Refined Holomorphic Anomaly Equation

The refined holomorphic anomaly equation for the topological string [18, 25] is given by

$$\bar{\partial}_i F^{(n_1, n_2)} = \frac{1}{2} \bar{C}_i^{jk} \left(D_j D_k F^{(n_1, n_2-1)} + \sum'_{m,h} D_j F^{(m,h)} \cdot D_k F^{(n_1-m, n_2-h)} \right) \quad (3.7)$$

¹⁵One can speculate that there is a subgroup of $\mathrm{SL}(2, \mathbb{R})$ which plays the role of the modular group on the sub-slice, but this would require to understand the relation of the fourth order differential equation (4.33) to a Schwarzian system along the lines discussed in [33].

for $n_1 + n_2 > 1$, where the prime mark indicates omission of terms with $(m, h) = (0, 0)$ and (n_1, n_2) . The indices i, j, k run over the number of different moduli of the curve. Covariant derivatives D_i correspond to the metric G_{ij} on the moduli space of complex structures of Σ_g . The metric can be expressed using the standard period matrix τ_{ij} of the standard holomorphic one-forms of Σ_g as

$$G_{i\bar{j}} = -i(\tau - \bar{\tau})_{ij} . \quad (3.8)$$

Furthermore, the expression \bar{C}_i^{jk} is related to the Yukawa coupling

$$C_{ijk} = \frac{\partial^3 F^{(0,0)}}{\partial t_i \partial t_j \partial t_k} \quad (3.9)$$

by

$$\bar{C}_i^{jk} = G^{l\bar{p}} G^{m\bar{n}} \bar{C}_{\bar{p}\bar{n}\bar{k}} . \quad (3.10)$$

Moreover, the Yukawa coupling can be given for example by

$$\frac{\partial \tau_{ij}}{\partial \nu_k} = C_i^m C_j^n C_{knm} , \quad (3.11)$$

where the invertible constant matrix C_i^m is given by a relative normalisation of the classical periods of the holomorphic one form differentials relative to the periods $\nu_i(\xi, \eta)$ and $\nu_{D_i}(\xi, \eta)$ as discussed in [25]. This means that the C_i^{jk} are given entirely in terms of the classical periods.

In (3.7) the anomaly equation is stated in its most general form. For the conjecture we have to restrict to the Nekrasov-Shatashvili (NS) limit [23] $n_2 = 0$ for which the first term of (3.7) drops out and we are left with the free energies

$$F_n = F^{(n,0)} . \quad (3.12)$$

3.4 Direct Integration Procedure in Terms of Propagators

Solving the anomaly equation can be done with the direct integration procedure [18, 20, 25]. Here we will use the direct integration method from [21], which is formulated in terms of the propagator S^{ij} , the latter being defined by

$$\bar{\partial}_{\bar{k}} S^{ij} = \bar{C}_{\bar{k}}^{ij} . \quad (3.13)$$

The idea of the direct integration method is to rewrite the anti-holomorphic derivatives as derivatives with respect to the propagator

$$\bar{\partial}_{\bar{i}} F^{(n_1, n_2)} = \bar{C}_{\bar{i}}^{jk} \frac{\partial F^{(n_1, n_2)}}{\partial S^{jk}} \quad (3.14)$$

such that (3.7) becomes¹⁶

$$\frac{\partial F^{(n_1, n_2)}}{\partial S^{jk}} = \frac{1}{2} \left(D_j \partial_k F^{(n_1, n_2-1)} + \sum'_{m, h} \partial_j F^{(m, h)} \cdot \partial_k F^{(n_1-m, n_2-h)} \right) . \quad (3.15)$$

¹⁶Here we have to assume that the $\bar{C}_{\bar{i}}^{jk}$ are linearly independent. Furthermore, the covariant derivatives become normal derivatives because in the local case the Kähler connection in the covariant derivatives becomes trivial.

The propagator can be calculated from a set of equations derived from special geometry of the moduli space [25]

$$\begin{aligned} D_i S^{kl} &= -C_{imn} S^{km} S^{ln} + f_i^{kl} , \\ \Gamma_{ij}^k &= -C_{ijl} S^{kl} + \tilde{f}_{ij}^k , \\ \partial_i F^{(0,1)} &= \frac{1}{2} C_{ijk} S^{jk} A_i . \end{aligned} \tag{3.16}$$

These equations are overdetermined in the multi-moduli case. In the one-parameter case we solve these equations by imposing $A_\xi = 0$. The other two ambiguities can then be fixed. As an ansatz for the unknowns in (3.16) one can choose

$$f_i^{kl} = \frac{h(\xi)}{\prod_r \Delta_r^p} , \tag{3.17}$$

where Δ_r are different factors of the discriminant and $h(\xi)$ is some polynomial in the modulus ξ . An analog ansatz is made for \tilde{f}_{ij}^k .

As initial values for the holomorphic anomaly equation a suitable form for $F^{(0,0)}$, $F^{(1,0)}$ and $F^{(0,1)}$ is demanded. From special geometry $F^{(0,0)}$ can be determined. For $F^{(1,0)}$ and $F^{(0,1)}$, respectively, we take [25]

$$\begin{aligned} F^{(1,0)} &= \frac{k_1}{24} \log(\Delta \xi^\alpha) \quad \text{and} \\ \mathcal{F}^{(0,1)} &= \frac{k'_1}{2} \log \left(\Delta^a \xi^b \cdot \left(\frac{\partial t}{\partial \xi} \right)^{-1} \right) \end{aligned} \tag{3.18}$$

as a suitable ansatz where the parameters α , a and b have to be fixed. By comparison with the WKB results we can fix these parameters. With $\mathcal{F}^{(0,1)}$ we refer to the holomorphic part of $F^{(0,1)}$. For our computations it is enough to specify the holomorphic part only. It is well known that the propagator in ν -coordinates can be given in terms of almost holomorphic modular forms [25], which for genus one read

$$\hat{S}^{\nu\nu} = \frac{c^2}{12} \left(E_2 - \frac{3}{\pi \text{Im}(\tau)} \right) = \frac{c^2}{12} \hat{E}_2 \tag{3.19}$$

while for genus two curves with $\text{Im}(\tau)_{pq}$, $p, q = 1, 2$ one obtains a very similar expression

$$\hat{S}^{ij} = \frac{1}{2\pi i} \frac{C_p^i C_q^j}{10} \left(\frac{\partial}{\partial \tau_{pq}} \log(\chi_{10}(\tau)) - \frac{5}{2\pi} (\text{Im}(\tau)^{-1})^{pq} \right) , \tag{3.20}$$

where now χ_{10} is the Igusa cusp form and the C_p^i are constant invertible normalisation matrices. For $\Sigma_{g>2}$ one can solve (3.16) to get further interesting anholomorphic objects. From the general structure one can see that solving (3.15) explicitly leads to $F^{(m,g)}$ that are polynomials of degree $3g+2n-3$ in the propagators with meromorphic but not an-holomorphic coefficients so that the total expression for $F^{(m,g)}$ is invariant on the monodromy group Γ_{Σ_g} of the family Σ_g . The meromorphic coefficients become simpler if one redefines the propagators themselves by meromorphic but not an-holomorphic forms, which we will do in section 4.1.3.

3.5 Fixing the Holomorphic Ambiguity

After integrating we still have a holomorphic ambiguity or recursion kernel in the free energies $F^{(n_1, n_2)}(\epsilon_1, \epsilon_2, \nu)$ or more specifically in the $F_n = F^{(n, 0)}$. Fixing this ambiguity can be done by imposing the so called gap condition at all conifold divisors with a suitable normalised vanishing cycle ν , at which the leading behavior of each $F^{(n_1, n_2)}(\epsilon_1, \epsilon_2, \nu)$ can be determined by an expansion the refined BPS saturated Schwinger-Loop integral

$$\begin{aligned}
F(s, g_s, \nu) &= \int_0^\infty \frac{d\sigma}{\sigma} \frac{\exp(-\sigma\nu)}{4 \sinh(\sigma\epsilon_1/2) \sinh(\sigma\epsilon_2/2)} + \mathcal{O}(\nu^0) \\
&= \left[-\frac{1}{12} + \frac{1}{24}(\epsilon_1 + \epsilon_2)^2(\epsilon_1\epsilon_2)^{-1} \right] \log(\nu) \\
&\quad + \frac{1}{\epsilon_1\epsilon_2} \sum_{g=0}^\infty \frac{(2g-3)!}{\nu^{2g-2}} \sum_{m=0}^g \hat{B}_{2g} \hat{B}_{2g-2m} \epsilon_1^{2g-2m} \epsilon_2^{2m} + \dots \\
&= \left[-\frac{1}{12} + \frac{1}{24} s g_s^{-2} \right] \log(\nu) + \left[-\frac{1}{240} g_s^2 + \frac{7}{1440} s - \frac{7}{5760} s^2 g_s^{-2} \right] \frac{1}{\nu^2} \\
&\quad + \left[\frac{1}{1008} g_s^4 - \frac{41}{20160} s g_s^2 + \frac{31}{26880} s^2 - \frac{31}{161280} s^3 g_s^{-2} \right] \frac{1}{\nu^4} + \mathcal{O}(\nu^0) \\
&\quad + \text{contributions to } 2(g+n) - 2 > 4.
\end{aligned} \tag{3.21}$$

Here $g_s^2 = (\epsilon_1\epsilon_2)$, $s = (\epsilon_1 + \epsilon_2)^2$ and $\hat{B}_m = \left(\frac{1}{2^{m-1}} - 1\right) \frac{B_m}{m!}$, where B_m are the Bernoulli numbers defined by the generating function $t/(e^t-1) = \sum_{m=0}^\infty B_m \frac{t^m}{m!}$. This determines the leading coefficient of the free energies and moreover implies that all other lower singular coefficients vanish. More precisely, the gap conditions, for example for the later defined sextic oscillator, can be written as

$$\begin{aligned}
F_n(\nu) &= k_n \frac{(1 - 2^{1-2n})(2n-3)! B_{2n}}{(2n)!} \nu^{2-2n} + \mathcal{O}(\nu^0) \quad \text{and} \\
F_n^\pm(t_f^\pm) &= k_n^\pm \frac{(1 - 2^{1-2n})(2n-3)! B_{2n}}{(2n)!} \cdot \left(-\frac{1}{2}\right) (-4)^n \left(t_f^\pm\right)^{2-2n} + \mathcal{O}\left(\left(t_f^\pm\right)^0\right)
\end{aligned} \tag{3.22}$$

where $n \geq 2$. In (3.22) ν and t_f^\pm label locally flat coordinates around the conifold loci associated to the vanishing cycles. In our model we could set the normalization constants k_n and k_n^\pm to unity. It is interesting that the upper gap condition is general in the sense that it is true for all anharmonic oscillators (4.1), not only for the sextic. This is related to the fact that the gap condition is implied by the quantization condition of the underlying quantum mechanical system [15, 34–36]. The asymptotic behavior implied by the quantization condition reads

$$\begin{aligned}
-\int \log \left[\frac{\sqrt{2\pi}}{\Gamma\left(\nu + \frac{1}{2}\right)} \right] d\nu &= \frac{\nu^2}{2} \left(\log \nu - \frac{3}{2} \right) - \frac{1}{24} \log \nu - \frac{7}{5760} \frac{1}{\nu^2} \\
&\quad + \frac{31}{161280} \frac{1}{\nu^4} - \frac{127}{1290240} \frac{1}{\nu^6} + \mathcal{O}\left(\frac{1}{\nu^8}\right)
\end{aligned} \tag{3.23}$$

and matches with the leading singular coefficient of the free energies. This universal singular behavior shows up for both examples we discuss in section 4.

The holomorphic ambiguity can be parametrized as a polynomial divided by the discriminant locus to the power $2n - 2$. The degree of the numerator is bounded imposing regularity for $\xi \rightarrow \infty$. Actually, the degree can be further reduced by one as the highest degree monomial can be combined with appropriate lower degree ones to yield a constant contribution in ξ . This gives a constant contribution to the free energies which is unphysical. More precisely, this means

$$h_n(\xi) = \frac{u_n(\xi)}{(\prod_r \Delta_r^p)^{2n-2}}, \quad (3.24)$$

where $u_n(\xi)$ is a polynomial whose degree is one less than that of the denominator. Requiring linear independence of the gap condition at all conifold loci fixes the holomorphic ambiguity completely.

4 Examples

Our two examples fall into the class of anharmonic oscillators of the form

$$V(x) = \frac{x^2}{2} - \mathfrak{g}x^d, \quad (4.1)$$

which has also been studied in e.g. [15, 34–38]. In this work we focus on the cases where the corresponding WKB curve has genus two, namely the quintic ($d = 5$) and symmetric sextic ($d = 6$) case. For any degree d the coupling \mathfrak{g} may be set to unity upon rescaling

$$x \rightarrow x \cdot \mathfrak{g}^{1/(2-d)}, \quad y \rightarrow y \cdot \mathfrak{g}^{1/(2-d)}, \quad \xi \rightarrow \xi \cdot \mathfrak{g}^{2/(2-d)} \quad (4.2)$$

so that ξ remains as single modulus of the hyperelliptic curve

$$\Sigma : \quad y^2 = 2\xi - x^2 + 2x^d. \quad (4.3)$$

For potentials of the simple form (4.1) the critical values can be computed explicitly and for all d . Solving the common root condition one finds

$$\Delta_d(\xi) = \xi \prod_{k=0}^{d-3} \left(\xi - v e^{2\pi i \frac{2k}{d-2}} \right) \quad \text{with} \quad v = \frac{d-2}{2} d^{\frac{d}{2-d}} > 0 \quad (4.4)$$

such that the non-zero roots of the discriminant differ by roots of unity. Examples with different d are shown in Fig. 4.1a, while Fig. 4.1b introduces homotopy generators relevant for monodromies using the example of the quintic.

It is clear that all WKB differentials are linear combinations of differentials $\frac{x^m}{y^k} dx$, $k = 3n - 1$. Their residues are given in appendix A for potentials of the form (4.1). Especially we give necessary conditions on k, m and d for non-zero residue. In all but

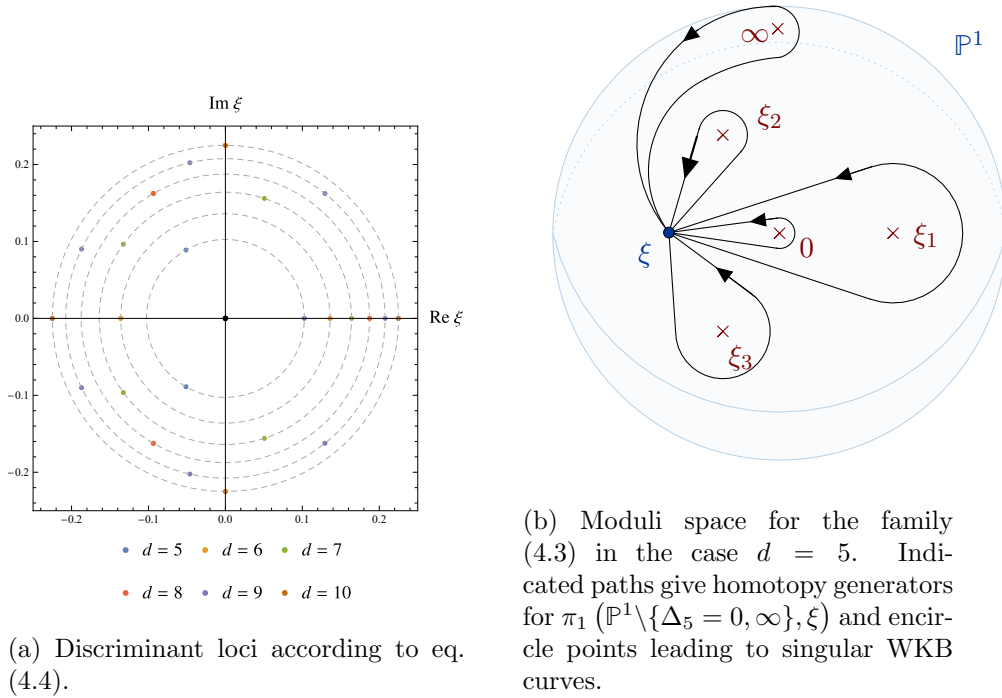


Figure 4.1: Moduli space for the family (4.3) in case of various degrees d .

one case these are not satisfied for the terms in \mathcal{Q}_{2n} due to (2.19) and (2.20). For $n \geq 1$ the residue of \mathcal{Q}_{2n} at the point(s) at infinity vanishes, independent of $d > 2$. Regarding the classical differential one finds

$$\text{Res}_{\infty^\pm} \mathcal{Q}_0 = \begin{cases} 0 & \text{if } d \neq 6 \text{ is even or } d \text{ is odd} \\ \frac{\pm 1}{2\sqrt{2}} & \text{if } d = 6. \end{cases} \quad (4.5)$$

Furthermore, the WKB differentials \mathcal{Q}_{2n} have no residues at the branch points. So except for the case¹⁷ $d = 6, n = 0$ all \mathcal{Q}_{2n} are differentials of the second kind and represent elements of $H^1(\Sigma, \mathbb{C})$.

4.1 The Symmetric Sextic Oscillator

The corresponding WKB curve

$$\Sigma^{(6)} : \quad y^2 = 2\xi - x^2 + 2x^6 = \prod_{k=1}^3 (x^2 - x_k^2) \quad (4.6)$$

is of genus $g = 2$. A plot of the potential as well as the homology cycles corresponding to pairs of real turning points are given in Fig. 4.2 for generic small $\xi > 0$. Over

¹⁷In this case the derivative $\partial_{\xi} y \, dx = y^{-1} \, dx$ is holomorphic.

the complex numbers there are always six turning points, two of which are complex conjugated. This is illustrated in Fig. 4.3 for ξ varying between two non-negative roots of the (normalized) discriminant

$$\Delta_6(\xi) = \xi (54\xi^2 - 1)^2. \quad (4.7)$$

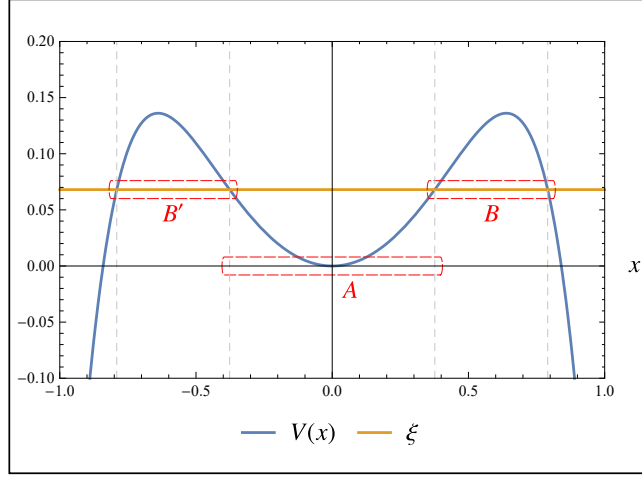


Figure 4.2: Sextic anharmonic potential with A - and B -cycle encircling pairs of turning points. The cycle B' is the image of B under $x \mapsto -x$.

4.1.1 Picard-Fuchs Operators and Quantum Differential Operators

To begin our discussion of the sextic oscillator we introduce quantum A - and B -periods $(\nu(\xi), \nu_D(\xi))$ as defined in (3.2) and (3.3). The A - and B -cycle are defined in Fig. 4.2 and encircle pairs of real branch points, see also Fig. 4.3. They are normalized such that $\nu^{(0)} = \xi + \dots$. The leading behavior of the classical periods can be determined as outlined in appendix B. Higher terms in the ξ -expansion are then generated using the Picard-Fuchs operator

$$\mathcal{L}_{\text{PF}}^{(0)} = \xi (54\xi^2 - 1) \partial_\xi^4 + 2 (162\xi^2 - 1) \partial_\xi^3 + 354\xi \partial_\xi^2 + 30 \partial_\xi. \quad (4.8)$$

Subsequently, quantum corrections to both periods are obtained by applying differential operators $\hbar^{2n} \mathcal{D}_{2n}$ to the classical periods $(\nu^{(0)}, \nu_D^{(0)})$, for example

$$\begin{aligned} \mathcal{D}_2 &= -\frac{45}{8} \xi \partial_\xi + \left(\frac{13}{45} - \frac{315}{8} \xi^2 \right) \partial_\xi^2 - \frac{5}{16} (-1 + 54\xi^2) \xi \partial_\xi^3 \\ \mathcal{D}_4 &= \frac{7 + 5670\xi^2}{192\xi - 10368\xi^3} \partial_\xi + \frac{2033 + 247050\xi^2}{960 - 51840\xi^2} \partial_\xi^2 + \frac{7 - 5724\xi^2 - 364500\xi^4}{2880\xi(-1 + 54\xi^2)} \partial_\xi^3. \end{aligned} \quad (4.9)$$

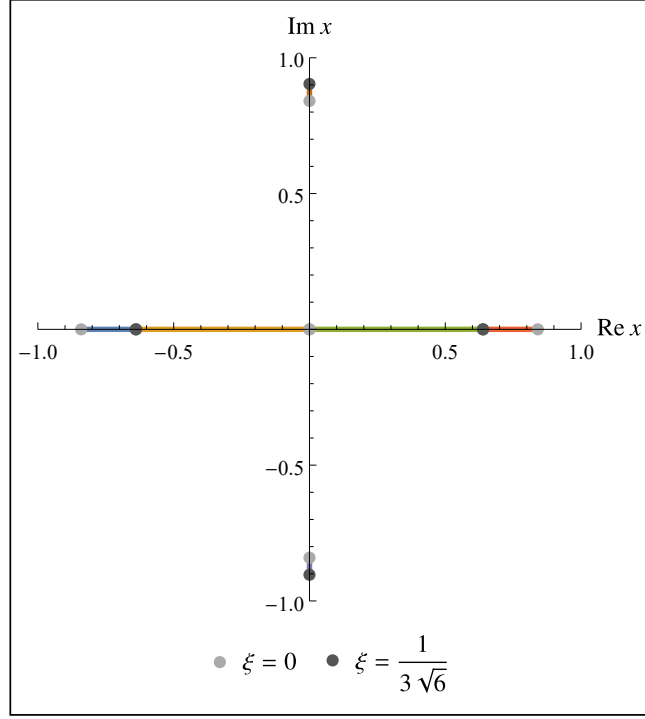


Figure 4.3: Trajectories of the turning points $x_i(\xi)$ as $\xi \in (0, \frac{1}{3\sqrt{6}})$ is varied between two zeroes of Δ_6 . Colors distinguish the six trajectories.

This leads to the following expansions for the first few WKB orders of the A -period

$$\begin{aligned}
 \nu^{(0)}(\xi) &= \xi + \frac{5}{2}\xi^3 + \frac{693}{16}\xi^5 + \frac{36465}{32}\xi^7 + \mathcal{O}(\xi^9) \\
 \nu^{(2)}(\xi) &= \frac{25}{8}\xi + \frac{5145}{32}\xi^3 + \frac{1096095}{128}\xi^5 + \mathcal{O}(\xi^7) \\
 \nu^{(4)}(\xi) &= \frac{21777}{256}\xi + \frac{8703695}{512}\xi^3 + \frac{16457464023}{8192}\xi^5 + \mathcal{O}(\xi^7) \\
 \nu^{(6)}(\xi) &= \frac{12746305}{2048}\xi + \frac{49058686105}{16384}\xi^3 + \frac{42777946276065}{65536}\xi^5 + \mathcal{O}(\xi^7) ,
 \end{aligned} \tag{4.10}$$

respectively the B -period

$$\begin{aligned}
\nu_D^{(0)}(\xi) &= \frac{\pi}{4\sqrt{2}} - \left(1 - \log\left(\frac{\xi}{2^{3/2}}\right)\right) \xi + \left(\frac{17}{3} + \frac{5}{2} \log\left(\frac{\xi}{2^{3/2}}\right)\right) \xi^3 + \mathcal{O}(\xi^5) \\
\nu_D^{(2)}(\xi) &= -\frac{1}{24} \frac{1}{\xi} + \left(\frac{149}{16} + \frac{25}{8} \log\left(\frac{\xi}{2^{3/2}}\right)\right) \xi + \left(\frac{62223}{128} + \frac{5145}{32} \log\left(\frac{\xi}{2^{3/2}}\right)\right) \xi^3 + \mathcal{O}(\xi^5) \\
\nu_D^{(4)}(\xi) &= \frac{7}{2880} \frac{1}{\xi^3} + \frac{43}{384} \frac{1}{\xi} + \left(\frac{1724749}{5120} + \frac{21777}{256} \log\left(\frac{\xi}{2^{3/2}}\right)\right) \xi \\
&\quad + \left(\frac{366995597}{6144} + \frac{8703695}{512} \log\left(\frac{\xi}{2^{3/2}}\right)\right) \xi^3 + \mathcal{O}(\xi^5) \\
\nu_D^{(6)}(\xi) &= -\frac{31}{40320} \frac{1}{\xi^5} - \frac{425}{32256} \frac{1}{\xi^3} - \frac{32793}{14336} \frac{1}{\xi} + \left(\frac{4824402623}{86016} + \frac{12746305}{1024} \log\left(\frac{\xi}{2^{3/2}}\right)\right) \xi \\
&\quad + \left(\frac{31906379165357}{2752512} + \frac{49058686105}{16384} \log\left(\frac{\xi}{2^{3/2}}\right)\right) \xi^3 + \mathcal{O}(\xi^5).
\end{aligned} \tag{4.11}$$

At any given order in \hbar^2 the A - and B -period are annihilated by a corresponding Picard-Fuchs operator which we collect in appendix C.

4.1.2 Quantum Free Energies from Quantum Mechanics

As explained in subsection 3.1 we can construct quantum free energies in the WKB framework. This is done by firstly computing the quantum periods (4.10) and (4.11), secondly using the inverse of the A -period as the mirror map to express the B -period in terms of ν and thirdly integrating with respect to ν . Thus, calculating free energies up to F_n requires the computation of the A - and B -period up to order \hbar^{2n} . We find

$$\begin{aligned}
F_0(\nu) &= \frac{\nu^2}{2} \left(\log\left(\frac{\nu}{2^{3/2}}\right) - \frac{3}{2}\right) + \frac{\pi}{4\sqrt{2}} \nu + \frac{17}{12} \nu^4 + \frac{10727}{960} \nu^6 + \frac{55747}{336} \nu^8 + \mathcal{O}(\nu^{10}) \\
F_1(\nu) &= -\frac{1}{24} \log \nu + \frac{221}{48} \nu^2 + \frac{38459}{384} \nu^4 + \frac{3442219}{1152} \nu^6 + \frac{2484506287}{24576} \nu^8 + \mathcal{O}(\nu^{10}) \\
F_2(\nu) &= -\frac{7}{5760} \frac{1}{\nu^2} + \frac{2283899}{15360} \nu^2 + \frac{14725045}{1152} \nu^4 + \frac{2619604188383}{2949120} \nu^6 \\
&\quad + \frac{284059718609}{5120} \nu^8 + \mathcal{O}(\nu^{10}) \\
F_3(\nu) &= \frac{31}{161280 \nu^4} + \frac{1642757413 \nu^2}{129024} + \frac{3084767116889 \nu^4}{1179648} + \frac{334449226613647 \nu^6}{983040} \\
&\quad + \frac{191100242149408097 \nu^8}{5505024} + \mathcal{O}(\nu^{10}).
\end{aligned} \tag{4.12}$$

These expressions can be compared with the topological string computation which we will be presented shortly. As initial datum we use the classical free energy $F_0(\nu)$. Moreover, the first quantum correction F_1 will be used to fix the parameters in the ansatz (3.18).

4.1.3 Solving the Holomorphic Anomaly Equation for the Reduced Sextic

So far, we have used geometry within the WKB method to calculate quantum periods. On the other hand using the claim stated in subsection 3.1 we can use string theoretical methods, namely the holomorphic anomaly equation, to compute free energies related to quantum periods by (3.5). In this paragraph we make this explicit by solving the holomorphic anomaly equation for the sextic curve (4.6). Our approach to solve this equation follows the procedure in [21].

Starting with the classical free energy F_0 (4.12) we can compute the Yukawa coupling (4.13) in the coordinate ξ as

$$C_{\xi\xi\xi} = \frac{1}{\xi(1-54\xi^2)} . \quad (4.13)$$

By comparison with the quantum mechanical computations (4.12) we can fix the parameters in (3.18) and find for F_1

$$F_1 = -\frac{1}{24} \log \left(\xi (1 - 54\xi^2)^2 \right) . \quad (4.14)$$

We can now compute the propagator from (3.16) imposing $A_\xi = 0$ and obtain

$$S^{\xi\xi} = -15\xi^2 + \frac{225}{4}\xi^4 + \frac{6975}{4}\xi^6 + \frac{8253225}{128}\xi^8 + \mathcal{O}(\xi^{10}) . \quad (4.15)$$

As it turns out, the parameters a and b in the ansatz (3.18) for $\mathcal{F}^{(0,1)}$ may be set to zero as they will only affect the constant terms of the free energies which in our case are unphysical since the WKB method only determines the derivative of the free energies. Then the Christoffel symbols and the covariant derivative of the propagator are given by

$$\begin{aligned} \Gamma_{\xi\xi}^\xi &= -C_{\xi\xi\xi} S^{\xi\xi} & \text{and} \\ D_\xi S^{\xi\xi} &= -C_{\xi\xi\xi} S^{\xi\xi} S^{\xi\xi} - 30\xi . \end{aligned} \quad (4.16)$$

By considering NS free energies the first part in (3.15) drops out. After writing everything as a polynomial in the propagator with coefficients being rational functions in ξ we obtain

$$F_2 = \frac{(1 - 270\xi^2)^2}{1152\xi^2 (1 - 54\xi^2)^2} S^{\xi\xi} + h_2(\xi) . \quad (4.17)$$

The holomorphic ambiguity $h_2(\xi)$ can be fixed by the gap condition at all three conifold loci

$$\Delta = \xi (1 - 54\xi^2)^2 = 0 \quad \Rightarrow \quad \xi_c \in \left\{ 0, \pm \frac{1}{\sqrt{54}} \right\} . \quad (4.18)$$

The propagator is transformed to a different conifold locus with

$$S_f^{\xi\xi} = \frac{2}{C_{\xi\xi\xi}} \partial_\xi \mathcal{F}_f^{(0,1)} = \frac{1}{C_{\xi\xi\xi}} \partial_\xi \log \left(\frac{\partial \xi}{\partial t_f} \right) , \quad (4.19)$$

where t_f is an appropriate flat coordinate at the conifold loci. Imposing the gap condition at these three points is enough to fix the ambiguity completely. If we assume that the gap conditions give linearly independent conditions we will obtain $6(n-1)$ conditions, which equals the number of parameters in the ambiguity (3.24). The result for h_2 reads

$$h_2(\xi) = \frac{-7 + 3924\xi^2 + 461700\xi^4}{5760\xi^2(1 - 54\xi^2)^2}. \quad (4.20)$$

Expanding at the conifold locus $\xi_c = 0$ in the flat coordinate ν we find¹⁸

$$F_2 = \frac{7}{5760} \frac{1}{\nu^2} + \frac{2283899}{15360} \nu^2 + \frac{14725045}{1152} \nu^4 + \frac{2619604188383}{2949120} \nu^6 + \mathcal{O}(\nu^8). \quad (4.21)$$

For the higher free energies we can now go on and compute them recursively. For F_3 we find

$$\begin{aligned} F_3 = & \frac{-1 + 270\xi^2}{414720\xi^4(1 - 54\xi^2)^4} (42 - 7254\xi + 5580252\xi^4 + 103663800\xi^6 + 1771470000\xi^8 \\ & - 15S^{\xi\xi} + 2430\xi^2 S^{\xi\xi} + 218700\xi^4 S^{\xi\xi} + 59049000\xi^6 S^{\xi\xi} + 5(S^{\xi\xi})^2 - 2700\xi^2 (S^{\xi\xi})^2 \\ & + 364500\xi^4 (S^{\xi\xi})^2) \\ & + \frac{31 - 7251\xi^2 + 3442320\xi^4 + 1396047960\xi^6 + 44918355600\xi^8 + 296780274000\xi^{10}}{161280\xi^4(1 - 54\xi^2)^4}. \end{aligned} \quad (4.22)$$

Expressing higher free energies at the conifold locus $\xi_c = 0$ as well in terms of the locally flat coordinate ν we recover quantum mechanical results.

We checked with explicit computations in the WKB framework as well as in the topological string framework that up to order \hbar^{10} the free energies agree. This provides a constructive confirmation of the conjecture proposed in [15], at least with regard to the current example. Moreover, the gap condition at all conifold loci gives enough information to fix the holomorphic ambiguities completely.

From a computational point of view solving the holomorphic anomaly equation is more involved. The geometrical methods used to compute quantum periods are more efficient. In particular, using quantum differential operators \mathcal{D}_{2n} simplifies and accelerates the calculation of the quantum periods enormously. With a modern computer quantum differential operators can be computed quickly.

4.1.4 Reduction to the Elliptic Case

A special property of the symmetric sextic potential is that all WKB periods along A, B and B' reduce to elliptic ones.

To see this, first consider the Klein four-group $\mathbb{Z}_2 \times \mathbb{Z}_2 \subset \text{Aut}(\Sigma^{(6)})$ of holomorphic automorphisms generated by the hyperelliptic involution $i_1 : (y, x) \mapsto (-y, x)$ and the reflection $i_2 : (y, x) \mapsto (y, -x)$. The involution $i_3 = i_2 i_1$ simultaneously reversing

¹⁸Here and in the following we have dropped the unphysical constant term.

position and momentum has no fixed points, as for $\xi \neq 0$ none of the branch points $(0, x_k)$ equals $(0, 0)$. Hence it defines an unramified two-sheeted covering¹⁹

$$c : \begin{cases} \Sigma^{(6)} & \rightarrow & \Sigma^{(6)}/i_3 \\ (y, x) & \mapsto & (Y, X) = (yx, x^2) \end{cases} \quad (4.23)$$

mapping to the elliptic curve $\mathcal{E} = \Sigma^{(6)}/i_3$ given by

$$\mathcal{E} : Y^2 = X \prod_{i=k}^3 (X - x_k^2) . \quad (4.24)$$

Even though $\Sigma^{(6)}$ may also be regarded as double covering of the elliptic curve $\Sigma^{(6)}/i_2 : y^2 = 2\xi - X + 2X^3$, this is not the correct geometry for the WKB periods: naïve substitution in the classical differential $y \, dx$ leads to the tentative one-form

$$\sqrt{2\xi - X + 2X^3} \frac{dX}{2\sqrt{X}} , \quad (4.25)$$

which however is multi-valued in any sheet of $\Sigma^{(6)}/i_2$ (note that $(y, X = 0)$ is not a branch point). Expanding the fraction by \sqrt{X} , we obtain the one-form $\omega = Y \, dX/2X$ well-defined on $\Sigma^{(6)}/i_3$.

By mathematical induction it can then be shown that all WKB differentials $\mathcal{Q}_n = Q_n(x) \, dx$ may be written as $\mathcal{Q}_n = p_n(x) \, dx/y^{3n-1}$ with polynomials $p_n(x) = (-1)^n p_n(-x)$ of well-defined parity (given that the potential $V(x)$ is an even polynomial). Thus, they are invariant under the action of i_3 ,

$$i_3^* \mathcal{Q}_n = \frac{p_n(-x) \, d(-x)}{(-y)^{3n-1}} = \mathcal{Q}_n \quad (4.26)$$

and there exist polynomials $\tilde{p}_n(X)$ such that all WKB differentials become pullbacks of meromorphic forms on \mathcal{E} ,

$$\mathcal{Q}_n = c^* \left(\frac{\tilde{p}_n(X) \, dX}{Y^{3n-1}} \right) . \quad (4.27)$$

Note that the holomorphic one-form $Y^{-1} \, dX = \partial_\xi \omega$ on \mathcal{E} corresponds to its pullback $y^{-1} \, dx = \partial_\xi (y \, dx)$ on Σ .

As the space $H_1(\mathcal{E}, \mathbb{C})$ has smaller dimension than $H_1(\Sigma, \mathbb{C})$, we need to check that the classical A - and B -periods on the sextic (and thus their quantum counterparts) map to periods on \mathcal{E} . One way to verify this is to note that the Picard-Fuchs operator for the one-form ω reads

$$\mathcal{L}_\mathcal{E}^{(0)} = \xi(54\xi^2 - 1) \partial_\xi^3 + (162\xi^2 - 1) \partial_\xi^2 + 30\xi \partial_\xi \quad (4.28)$$

¹⁹This makes use of the following theorem [39]: Let \mathcal{R} be a (compact) Riemann surface and G be a finite group of holomorphic automorphisms of order $|G|$. Then \mathcal{R}/G is a Riemann surface with the complex structure determined by the condition that the canonical projection $\pi : \mathcal{R} \rightarrow \mathcal{R}/G$ is holomorphic. This is a $|G|$ -sheeted covering, ramified at the fixed points of G .

and annihilates

$$\begin{aligned}\nu^{(0)}(\xi) &= \xi {}_3F_2\left(\frac{1}{6}, \frac{1}{2}, \frac{5}{6}; 1, \frac{3}{2}; 54\xi^2\right) \\ &= \xi + \frac{5\xi^3}{2} + \frac{693\xi^5}{16} + \frac{36465\xi^7}{32} + \frac{37182145\xi^9}{1024} + \mathcal{O}(\xi^{11})\end{aligned}\quad (4.29)$$

as well as

$$\begin{aligned}\nu_D^{(0)}(\xi) &= \frac{\pi}{2^{5/2}} - \frac{\pi}{2} \xi G_{3,3}^{2,1}\left(54\xi^2 \left| \begin{matrix} \frac{1}{2}, \frac{1}{6}, \frac{5}{6} \\ 0, 0, -\frac{1}{2} \end{matrix} \right. \right) \\ &= \frac{\pi}{4\sqrt{2}} + \log\left(\frac{\xi}{2^{3/2}}\right) \left(\xi + \frac{5\xi^3}{2} + \frac{693\xi^5}{16} + \frac{36465\xi^7}{32} + \frac{37182145\xi^9}{1024} + \mathcal{O}(\xi^{11})\right) \\ &\quad - \xi + \frac{17\xi^3}{3} + \frac{18027\xi^5}{160} + \frac{1394891\xi^7}{448} + \frac{3751204337\xi^9}{36864} + \mathcal{O}(\xi^{11}).\end{aligned}\quad (4.30)$$

This leads precisely to the subsystem spanned by the classical periods in (4.10) and (4.11) and the residue of $(y \, dx, \Sigma)$ or (ω, \mathcal{E}) . One can also check these findings by explicit computation of periods on \mathcal{E} .

4.2 The Quintic Oscillator

We now turn to the quintic potential, $d = 5$, which leads to the family of genus-two curves

$$\Sigma_{(5)} : \quad y^2 = 2\xi - x^2 + 2x^5. \quad (4.31)$$

The quintic curve can not be regarded as multi-cover of an elliptic curve and is in this sense more generic. The potential and the homology cycles corresponding to pairs of real turning points are given in Fig. 4.4 for generic small $\xi > 0$. Moreover, in Fig. 4.5 the movement of the branch points is visualized. There are three real branch points and one pair of complex conjugated branch points. Additionally one branch point is at infinity. The quintic curve gets singular if the moduli ξ is tuned to a root of the normalized discriminant

$$\Delta_5(\xi) = \xi (25000\xi^3 - 27). \quad (4.32)$$

4.2.1 Picard-Fuchs Operators and Quantum Differential Operators

The quantum periods ν and ν_D are defined by equation (3.2) and (3.3), with the A - and B -cycle encircling branch points as shown in Fig. 4.4 and 4.5. Classical periods can be determined from the Picard-Fuchs operator

$$\begin{aligned}\mathcal{L}_{\text{PF}}^{(0)} &= (\xi(25000\xi^3 - 27) \partial_\xi^4 + (6400000\xi^3 - 1728) \partial_\xi^3 + 10160000\xi^2 \partial_\xi^2 \\ &\quad + 1120000\xi \partial_\xi + 104720),\end{aligned}\quad (4.33)$$

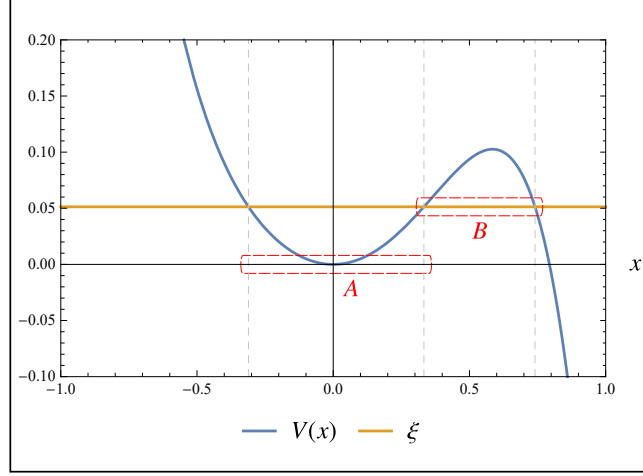


Figure 4.4: Quintic anharmonic potential with A - and B -cycle encircling pairs of turning points.

together with the leading behavior of the classical periods, which is determined in appendix B. Quantum corrections to the classical periods are easily obtained by applying differential operators $\hbar^{2n}\mathcal{D}_{2n}$ to the classical periods $(\nu^{(0)}, \nu_D^{(0)})$, for example

$$\begin{aligned} \mathcal{D}_2 &= -\frac{5}{567} (25000\xi^3 - 27) \xi \partial_\xi^3 - \left(\frac{11}{56} - \frac{137500}{189} \xi^3 \right) \partial_\xi^2 - \frac{8750}{81} \xi^2 \partial_\xi^1 - \frac{1375}{81} \xi \partial_\xi^0 \\ \mathcal{D}_4 &= -\frac{(39500000000\xi^6 + 89640000\xi^3 - 5103)}{77760\xi(25000\xi^3 - 27)} \partial_\xi^3 - \frac{125\xi(31900000\xi^3 + 37557)}{2592(25000\xi^3 - 27)} \partial_\xi^2 \\ &\quad - \frac{5(172100000\xi^3 + 111807)}{3888(25000\xi^3 - 27)} \partial_\xi^1 - \frac{9163(200000\xi^3 + 27)}{62208\xi(25000\xi^3 - 27)} \partial_\xi^0. \end{aligned} \quad (4.34)$$

The first few WKB orders of the quantum A -period read

$$\begin{aligned} \nu^{(0)}(\xi) &= \xi + \frac{315}{16} \xi^4 + \frac{692835}{128} \xi^7 + \frac{9704539845}{4096} \xi^{10} + \mathcal{O}(\xi^{13}) \\ \nu^{(2)}(\xi) &= \frac{1085}{32} \xi^2 + \frac{15570555}{512} \xi^5 + \frac{456782651325}{16384} \xi^8 + \frac{6734319857340075}{262144} \xi^{11} + \mathcal{O}(\xi^{14}) \\ \nu^{(4)}(\xi) &= \frac{1107}{256} + \frac{96201105}{2048} \xi^3 + \frac{4140194663605}{32768} \xi^6 + \frac{489884540580510075}{2097152} \xi^9 + \mathcal{O}(\xi^{12}) \\ \nu^{(6)}(\xi) &= \frac{118165905}{8192} \xi + \frac{30926063193025}{131072} \xi^4 + \frac{2364285204614844225}{2097152} \xi^7 \\ &\quad + \frac{223004451972549877775145}{67108864} \xi^{10} + \mathcal{O}(\xi^{13}) \end{aligned} \quad (4.35)$$

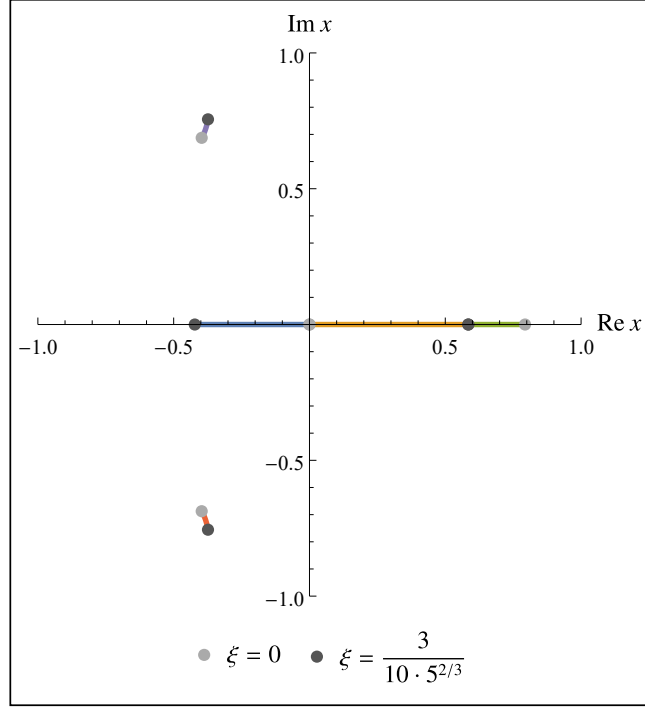


Figure 4.5: Trajectories of the turning points $x_i(\xi)$ as $\xi \in \left(0, \frac{3}{10 \cdot 5^{2/3}}\right)$ is varied between two zeroes of Δ_5 . Colors distinguish the five trajectories.

and respectively for the B -period

$$\begin{aligned}
\nu_D^{(0)}(\xi) &= \frac{\sqrt{\pi} \Gamma\left(\frac{5}{3}\right)}{2 \cdot 2^{2/3} \Gamma\left(\frac{13}{6}\right)} - \left(1 - \log\left(\frac{\xi}{2^{5/3}}\right)\right) \xi - \frac{7\pi \Gamma\left(-\frac{1}{3}\right)}{9 \Gamma\left(-\frac{1}{6}\right) \Gamma\left(\frac{5}{6}\right)} \xi^2 \\
&\quad + \frac{935\sqrt{\pi} \Gamma\left(\frac{2}{3}\right)}{324 \cdot 2^{2/3} \Gamma\left(\frac{7}{6}\right)} \xi^3 + \mathcal{O}(\xi^4) \\
\nu_D^{(2)}(\xi) &= -\frac{1}{24} \frac{1}{\xi} - \frac{11\sqrt{\pi} \Gamma\left(\frac{1}{3}\right)}{72 \cdot 2^{1/3} \Gamma\left(\frac{5}{6}\right)} + \frac{385\sqrt{\pi} \Gamma\left(\frac{2}{3}\right)}{24 \cdot 2^{2/3} \Gamma\left(\frac{1}{6}\right)} \xi + \left(\frac{66595}{576}\right. \\
&\quad \left. + \frac{1085}{32} \log\left(\frac{\xi}{2^{5/3}}\right)\right) \xi^2 + \mathcal{O}(\xi^3) \\
\nu_D^{(4)}(\xi) &= \frac{7}{2880} \frac{1}{\xi^3} + \left(\frac{16853}{768} + \frac{1107}{256} \log\left(\frac{\xi}{2^{5/3}}\right)\right) - \frac{4161703\sqrt{\pi} \Gamma\left(\frac{1}{3}\right)}{82944 \cdot 2^{1/3} \Gamma\left(\frac{5}{6}\right)} \xi \\
&\quad - \frac{450756 \cdot 2^{1/3} \sqrt{\pi} \Gamma\left(-\frac{7}{3}\right)}{150643225 \Gamma\left(-\frac{59}{6}\right)} \xi^2 + \mathcal{O}(\xi^3) \\
\nu_D^{(6)}(\xi) &= -\frac{31}{40320} \frac{1}{\xi^5} + \frac{53}{6144} \frac{1}{\xi^2} + \frac{1641726 \cdot 2^{1/3} \sqrt{\pi} \Gamma\left(-\frac{7}{3}\right)}{68542667375 \Gamma\left(-\frac{65}{6}\right)} + \left(\frac{8031474795}{114688}\right. \\
&\quad \left. + \frac{118165905}{8192} \log\left(\frac{\xi}{2^{5/3}}\right)\right) \xi + \frac{18570744 \cdot 2^{2/3} \sqrt{\pi} \Gamma\left(-\frac{11}{3}\right)}{490839606425 \Gamma\left(-\frac{85}{6}\right)} \xi^2 + \mathcal{O}(\xi^3).
\end{aligned} \tag{4.36}$$

It is interesting that transcendental numbers appear in the B -period. Comparing with the fundamental system²⁰ of the Picard-Fuchs operator for the classical periods

$$\begin{aligned}
\Pi_0(\xi) &= {}_4F_3 \left(-\frac{7}{30}, -\frac{1}{30}, \frac{11}{30}, \frac{17}{30}; \frac{1}{3}, \frac{2}{3}, \frac{2}{3}; \frac{25000\xi^3}{27} \right) \\
&= 1 + \frac{6545\xi^3}{648} + \frac{1682469481\xi^6}{839808} + \mathcal{O}(\xi^9) \\
\Pi_1(\xi) &= \xi {}_4F_3 \left(\frac{1}{10}, \frac{3}{10}, \frac{7}{10}, \frac{9}{10}; \frac{2}{3}, 1, \frac{4}{3}; \frac{25000\xi^3}{27} \right) \\
&= \xi + \frac{315\xi^4}{16} + \frac{692835\xi^7}{128} + \mathcal{O}(\xi^{10}) \\
\Pi_2(\xi) &= \xi^2 {}_4F_3 \left(\frac{13}{30}, \frac{19}{30}, \frac{31}{30}, \frac{37}{30}; \frac{4}{3}, \frac{4}{3}, \frac{5}{3}; \frac{25000\xi^3}{27} \right) \\
&= \xi^2 + \frac{283309\xi^5}{2592} + \frac{248945034845\xi^8}{6718464} + \mathcal{O}(\xi^{11}) \\
\Pi_{1'}(\xi) &= -\frac{1}{60\sqrt{3} 5^{2/3}\pi} G_{4,4}^{2,4} \left(\frac{25000\xi^3}{27} \left| \begin{array}{l} \frac{13}{30}, \frac{19}{30}, \frac{31}{30}, \frac{37}{30} \\ \frac{1}{3}, \frac{1}{3}, 0, \frac{2}{3} \end{array} \right. \right) \\
&= \log \left(\frac{\xi}{2^{5/3}} \right) \Pi_1(\xi) + \left[-\xi + \frac{10865\xi^4}{192} + \frac{78046343\xi^7}{4608} + \mathcal{O}(\xi^{10}) \right],
\end{aligned} \tag{4.37}$$

these transcendental numbers originate from the linear combinations for the B -period and not from the Picard-Fuchs equation itself. In particular, the A - and B -period are identified as follows

$$\begin{aligned}
\nu^{(0)}(\xi) &= \Pi_1(\xi) \\
\nu_D^{(0)}(\xi) &= \Pi_{1'}(\xi) + \frac{2^{1/3}\sqrt{\pi} \Gamma(\frac{2}{3})}{7 \Gamma(\frac{7}{6})} \Pi_0(\xi) - \frac{7\pi \Gamma(-\frac{1}{3})}{9 \Gamma(-\frac{1}{6}) \Gamma(\frac{5}{6})} \Pi_2(\xi).
\end{aligned} \tag{4.38}$$

These are essentially the only transcendental numbers appearing in this context as the coefficients at higher orders in \hbar come from the classical expressions using (4.34).

Picard-Fuchs equations for the A - and B -period at the first few orders in \hbar are summarized in appendix C.

²⁰The subscript indicates the corresponding root of the indicial equation.

4.2.2 Quantum Free Energies from Quantum Mechanics

As for the sextic oscillator we can compute quantum free energies. For the quintic we find

$$\begin{aligned}
F_0(\nu) &= \left(-\frac{3}{4} + \frac{1}{2} \log\left(\frac{\nu}{2^{5/3}}\right)\right) \nu^2 + \frac{2^{1/3} \sqrt{\pi} \Gamma\left(\frac{2}{3}\right)}{7 \Gamma\left(\frac{7}{6}\right)} \nu - \frac{7\pi \Gamma\left(-\frac{1}{3}\right)}{27 \Gamma\left(-\frac{1}{6}\right) \Gamma\left(\frac{5}{6}\right)} \nu^3 \\
&\quad + \frac{935 \sqrt{\pi} \Gamma\left(\frac{2}{3}\right)}{1296 \cdot 2^{2/3} \Gamma\left(\frac{7}{6}\right)} \nu^4 + \frac{2173}{192} \nu^5 + \mathcal{O}(\nu^6) \\
F_1(\nu) &= -\frac{1}{24} \log \nu - \frac{11 \sqrt{\pi} \Gamma\left(\frac{1}{3}\right)}{72 \cdot 2^{1/3} \Gamma\left(\frac{5}{6}\right)} \nu + \frac{385 \sqrt{\pi} \Gamma\left(\frac{2}{3}\right)}{48 \cdot 2^{2/3} \Gamma\left(\frac{1}{6}\right)} \nu^2 + \frac{132245}{3456} \nu^3 \\
&\quad - \frac{8527015 \pi \Gamma\left(-\frac{1}{3}\right)}{186624 \Gamma\left(-\frac{1}{6}\right) \Gamma\left(\frac{5}{6}\right)} \nu^4 + \mathcal{O}(\nu^5) \\
F_2(\nu) &= -\frac{7}{5760} \frac{1}{\nu^2} + \frac{21171}{1024} \nu - \frac{3882739 \sqrt{\pi} \Gamma\left(\frac{1}{3}\right)}{165888 \cdot 2^{1/3} \Gamma\left(\frac{5}{6}\right)} \nu^2 \\
&\quad - \frac{1599397248 \cdot 2^{1/3} \sqrt{\pi} \Gamma\left(-\frac{7}{3}\right)}{1708143528275 \Gamma\left(-\frac{59}{6}\right)} \nu^3 + \frac{3183085423}{73728} \nu^4 + \mathcal{O}(\nu^5) \\
F_3(\nu) &= \frac{31}{161280} \frac{1}{\nu^4} + \frac{3212061144326144 \sqrt[3]{2} \sqrt{\pi} \Gamma\left(-\frac{31}{3}\right)}{49809465284499 \Gamma\left(-\frac{65}{6}\right)} \nu + \frac{275141423}{8192} \nu^2 \\
&\quad + \frac{4068991173768 \cdot 2^{2/3} \sqrt{\pi} \Gamma\left(-\frac{11}{3}\right)}{351738173908023175 \Gamma\left(-\frac{85}{6}\right)} \nu^3 \\
&\quad + \frac{75795983236328485900 \sqrt[3]{2} \sqrt{\pi} \Gamma\left(-\frac{31}{3}\right)}{98404065562059 \Gamma\left(-\frac{65}{6}\right)} \nu^4 + \mathcal{O}(\nu^5)
\end{aligned} \tag{4.39}$$

which involve rational coefficients as well as transcendental ones. The structure of these transcendental numbers is inherited from the WKB periods. Topological string free energies are now highly constrained by this transcendental nature. It is one important step to recover these numbers in the string free energies. The leading singular coefficients of the free energies are the same as predicted from the gap condition (3.22).

4.2.3 Ansatz for F_1

For the topological string computation one necessary ingredient is a suitable ansatz for F_1 . According to equation (3.18) we make an ansatz in terms of the discriminant (4.32). Using the classical mirror map we can compare this ansatz to F_1 in (4.39). Unfortunately we obtain

$$\begin{aligned}
F_1^{\text{ansatz}}(\nu) &= -\frac{k_1}{24} (1 + \alpha) \log \nu \\
&\quad - k_1 \left(\frac{105\alpha}{128} + \frac{408505}{10368} \right) \nu^3 - k_1 \left(\frac{692255\alpha}{4096} + \frac{141101961685}{8957952} \right) \nu^6 + \mathcal{O}(\nu^9),
\end{aligned} \tag{4.40}$$

which can not fit with the WKB result. In particular, there are no powers of ν which have transcendental coefficients as in (4.39). Therefore, the ansatz (3.18) together with the classical mirror map can not reproduce WKB computations.

An ad hoc generalization of the form

$$F_1^{\text{ansatz}}(\nu) = p_1(\xi) + \alpha \log(p_2(\xi)) \quad (4.41)$$

where p_1 and p_2 are polynomials in ξ and α is a constant does not seem to work out. We tested this ansatz up to polynomials of order four and found no solution. This mismatch in the transcendental coefficients might suggest that one has to consider a system with monodromy in $\text{SL}(2, \mathbb{R})$ rather than the monodromy in $\text{SL}(2, \mathbb{Z})$ that arose in the problem with the symmetric sextic. Experience with the solution of the holomorphic anomaly for generic genus two hyperelliptic families [25] implies that the problem can be solved after a further deformation and strongly suggests that the transcendental coefficients come from the restriction to the sub-slice. We consider such a deformation in the next section and show that all quantum periods can be characterized by systems of two parameter differential operators \mathcal{D}_{2n} . However, comparing this result with a restriction of a solution of the genus two holomorphic anomaly equation is complicated and will be deferred to future work. Of course, such deformed quantum mechanical problems are in itself very interesting as they can for example exhibit competing vacua that will lead to new non-perturbative effects.

We have been informed by M. Mariño that at the Argyres-Douglas point²¹ of $\text{SU}(5)$ $\mathcal{N} = 2$ Yang-Mills theory one could obtain F_1 from the restriction of a genus four curve.

4.3 A Two-parameter Family of Quintic Curves

In this section we enhance our discussion of quantum periods to a true two-parameter higher-genus case²². The evaluation of hyperelliptic integrals becomes involved and laborious once more generic higher-genus curves are considered, which are *not* a multi-cover of an elliptic curve. This gets severe once (1.) quantum corrections are to be computed or (2.) integrands depend on more parameters than just the energy. We show that nevertheless our proposed formalism applies with minimal modification, thus highlighting its true strength. From a physics point of view this makes it possible to investigate systems very different in their classical behavior, i.e., the number of potential wells and thus oscillatory trajectories, on the common footing of their WKB quantum periods. Last but not least, we expect the embedding of the one-parameter quintic family (4.31) into a suitable two-parameter family to be a necessary step for the yet pending direct integration of the holomorphic anomaly recursion in case of a true genus-two geometry.

For concreteness, we study a parametric quintic potential with WKB curve

$$\Sigma^{(5')} : \quad y^2 = 2\xi - x^2 + 2x^5 + \eta(-x^2 + 2x^4) , \quad (4.42)$$

²¹Such points have been studied in the application to quantum mechanics in [16].

²²Recall that due to the rescaling symmetry (4.2) the parameter \mathfrak{g} accompanying leading monomials in (4.1) did not represent a true modulus of the WKB curve.

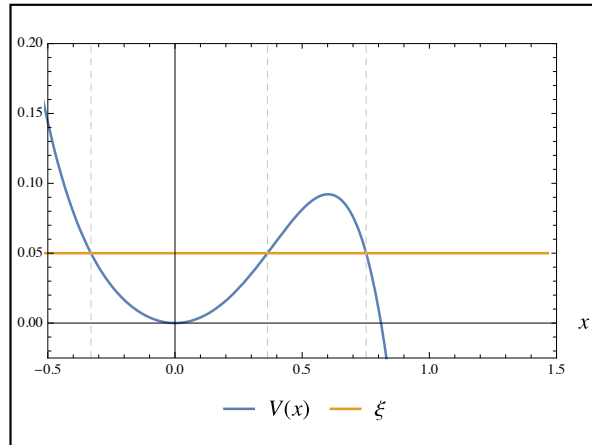


Figure 4.6: Perturbed quintic for $\eta = \frac{1}{10}$

where the coefficient of the leading monomial is again absorbed upon suitable rescaling. The perturbation is given by a quartic potential. The discriminant of $\Sigma_{5'}$ turns out to be

$$\Delta_{5'}(\xi, \eta) = \xi [25000\xi^3 + (1 + \eta)^4(-27 - 27\eta + 8\eta^3) + 64\xi^2\eta^2(-125 - 125\eta + 32\eta^3) - 4\xi\eta(1 + \eta)^2(-225 - 225\eta + 64\eta^3)] . \quad (4.43)$$

Note that still an explicit factorization according to (2.15) can be given, as the critical point condition is a quartic equation solvable in terms of radicals.

The perturbed quintic potential is visualized for different values of the perturbation parameter η in Figs. 4.6 - 4.8. Clearly, the number of real extrema changes from two to four as η is varied. For η sufficiently large one period integral previously belonging to a homology cycle around complex conjugated branch points now describes a physical action (at the classical level and for ξ as in Fig. 4.8).

The Picard-Fuchs operator \mathcal{L} generalizes in the two-parameter case to an ideal of Picard-Fuchs operators annihilating the periods. For the construction of operators generating the Picard-Fuchs ideal the ansatz in (2.22) gets extended including additional derivatives with respect to the second modulus η . Then the same procedure goes through, i.e., one subsequently eliminates monomials such that in the end one obtains the differential operator by imposing vanishing of the coefficients in front of the remaining monomials. In the two-parameter case there is an ambiguity in the vanishing condition. Independent choices of the free parameters yield a set of differential operators generating the Picard-Fuchs ideal.

For the perturbed quintic curve (4.42) there are two different Picard-Fuchs operators corresponding to two choices in the remaining parameters in the ansatz. Setting

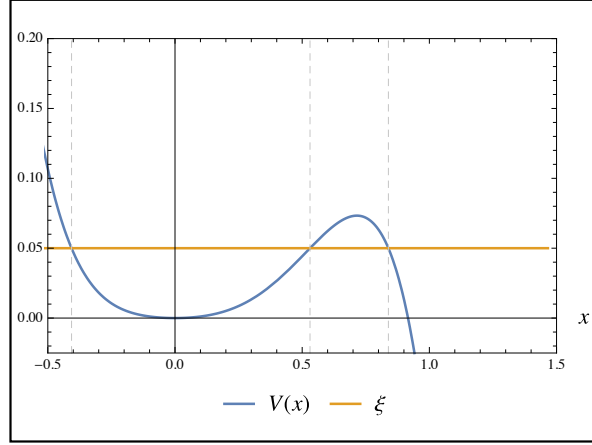


Figure 4.7: Perturbed quintic for $\eta \approx 0.4$

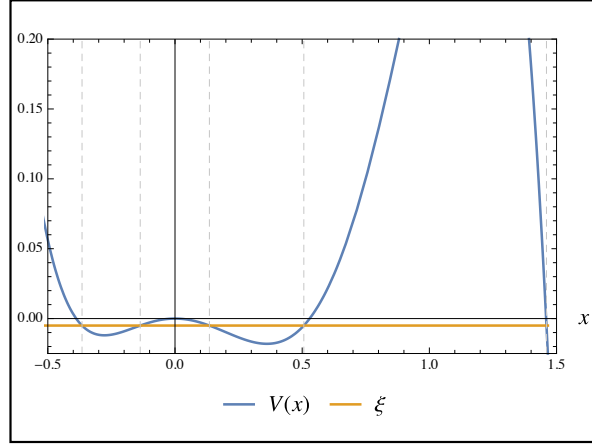


Figure 4.8: Perturbed quintic for $\eta = \frac{4}{5}$

them separately to unity we find

$$\begin{aligned}
\mathcal{L}_1 = & \left[-2\xi (320\eta (32\eta^3 - 75\eta - 50) \xi^2 + (56\eta^3 + 24\eta^2 - 135\eta - 135) (\eta + 1)^3 \right. \\
& \left. + 4(-384\eta^5 - 640\eta^4 + 644\eta^3 + 2025\eta^2 + 1350\eta + 225) \xi) \right] \partial_\xi^2 \\
& + \left[-2(24\eta^7 + \eta^6(96 - 512\xi) + \eta^5(2048\xi^2 - 1024\xi + 63) + \eta^4(1288\xi - 309) \right. \\
& \left. + \eta^3(-8000\xi^2 + 5400\xi - 786) - 10\eta^2(800\xi^2 - 540\xi + 81) + 45\eta(40\xi - 9) - 81) \right] \partial_\eta \partial_\xi \\
& + \left[-256\eta(4\eta^3 - 25\eta - 25) \xi^2 - 3(8\eta^3 - 27\eta - 27) (\eta + 1)^3 \right. \\
& \left. + 8(56\eta^5 + 64\eta^4 - 202\eta^3 - 465\eta^2 - 300\eta - 45) \xi \right] \partial_\xi \\
& + \left[8\eta(8\eta(16\eta^3 - 55\eta - 55) \xi - (\eta + 1)^2(8\eta^3 - 27\eta - 27)) \right] \partial_\eta \\
& + \left[224\eta(-16\eta^3 + 25\eta + 10) \xi + 14(16\eta^3 - 24\eta - 9) (\eta + 1)^2 \right]
\end{aligned}$$

$$\begin{aligned}
\mathcal{L}_2 = & [-2\xi (160 (352\eta^4 + 336\eta^3 - 650\eta^2 - 775\eta - 75) \xi^2 + (288\eta^4 + 664\eta^3 + 12\eta^2 \\
& - 999\eta - 675) (\eta + 1)^2 - 4 (2032\eta^5 + 5256\eta^4 + 1118\eta^3 - 7721\eta^2 - 7350\eta - 1575) \xi)] \partial_\xi^2 \\
& + [-6 (128\eta (16\eta^4 + 8\eta^3 - 75\eta^2 - 125\eta - 50) \xi^2 + (32\eta^4 + 40\eta^3 - 108\eta^2 \\
& - 243\eta - 135) (\eta + 1)^3 - 8 (80\eta^6 + 184\eta^5 - 178\eta^4 - 962\eta^3 - 1115\eta^2 - 480\eta - 45) \xi)] \partial_\eta \partial_\xi \\
& + [8\eta(2\eta + 3) (8\eta (16\eta^3 - 55\eta - 55) \xi - (\eta + 1)^2 (8\eta^3 - 27\eta - 27))] \partial_\eta^2 \\
& + [-64 (128\eta^4 - 96\eta^3 - 800\eta^2 - 875\eta - 75) \xi^2 - 3 (32\eta^4 + 40\eta^3 - 108\eta^2 \\
& - 243\eta - 135) (\eta + 1)^2 + 8 (256\eta^5 + 320\eta^4 - 1052\eta^3 - 2613\eta^2 - 1905\eta - 360) \xi] \xi \partial_\xi \\
& + [-70(2\eta + 3) (8 (16\eta^3 - 7\eta - 1) \xi - (\eta + 1)^2 (8\eta^2 - 3))] .
\end{aligned} \tag{4.44}$$

With an obvious extension of the Frobenius method allowing for a double power series ansatz in (2.24) and (2.25) and possibly logarithms in the new parameter η the periods are given by three pure power series

$$\begin{aligned}
\Pi_0(\xi, \eta) = & 1 - \frac{7}{8}\eta^2 - \frac{245}{648}\eta^3 + \mathcal{O}(\eta^4) \\
& + \left(\frac{7}{9}\eta - \frac{35}{108}\eta^2 + \frac{35}{162}\eta^3 + \mathcal{O}(\eta^4) \right) \xi \\
& + \left(-\frac{245}{72} + \frac{3185}{432}\eta - \frac{54355}{5184}\eta^2 + \mathcal{O}(\eta^3) \right) \xi^2 \\
& + \left(\frac{6545}{648} - \frac{271565}{3888}\eta + \frac{10417015}{46656}\eta^2 + \mathcal{O}(\eta^3) \right) \xi^3 + \mathcal{O}(\xi^4) \\
\Pi_1(\xi, \eta) = & \left(1 - \frac{1}{2}\eta + \frac{3}{8}\eta^2 - \frac{5}{16}\eta^3 + \mathcal{O}(\eta^4) \right) \xi \\
& + \left(\frac{3}{2}\eta - \frac{15}{4}\eta^2 + \frac{105}{16}\eta^3 + \mathcal{O}(\eta^4) \right) \xi^2 \\
& + \left(\frac{35}{4}\eta^2 - \frac{315}{8}\eta^3 + \mathcal{O}(\eta^4) \right) \xi^3 \\
& + \left(\frac{315}{16} - \frac{3465}{32}\eta + \frac{45045}{128}\eta^2 + \mathcal{O}(\eta^3) \right) \xi^4 + \mathcal{O}(\xi^5) \\
\Pi_2(\xi, \eta) = & \eta + \frac{5}{6}\eta^2 - \frac{5}{72}\eta^3 + \mathcal{O}(\eta^4) \\
& + \left(-\frac{5}{18}\eta^2 + \frac{35}{108}\eta^3 + \mathcal{O}(\eta^4) \right) \xi \\
& + \left(\frac{35}{12} - \frac{455}{72}\eta + \frac{8645}{864}\eta^2 + \mathcal{O}(\eta^3) \right) \xi^2 \\
& + \left(\frac{8645}{324}\eta - \frac{216125}{1944}\eta^2 + \frac{6699875}{23328}\eta^3 + \mathcal{O}(\eta^4) \right) \xi^3 \\
& + \left(\frac{6699875}{23328}\eta^2 - \frac{247895375}{139968}\eta^3 + \mathcal{O}(\eta^4) \right) \xi^4 + \mathcal{O}(\xi^5)
\end{aligned} \tag{4.45}$$

and a logarithmic solution

$$\begin{aligned}
\Pi_{1'}(\xi, \eta) &= \Pi_1(\xi, \eta) \cdot \log\left(\frac{\xi}{2^{5/3}}\right) + \left(\frac{1}{3}\eta^2 + \frac{1}{6}\eta^3 + \mathcal{O}(\eta^4)\right) \\
&+ \left(-1 - \frac{7}{6}\eta + \frac{31}{24}\eta^2 + \mathcal{O}(\eta^3)\right) \xi \\
&+ \left(\frac{53}{12}\eta - \frac{325}{24}\eta^2 + \frac{2575}{96}\eta^3 + \mathcal{O}(\eta^4)\right) \xi^2 + \mathcal{O}(\xi^3) .
\end{aligned} \tag{4.46}$$

As a consistency check setting the perturbation parameter η to zero restores the old fundamental system (4.37).

As in the one-parameter case it is possible to construct quantum operators which applied to the classical periods give the quantum periods. In the two-parameter case these quantum differential operators have some freedom. In the construction (2.26) we used that the cohomology group $H^1(\Sigma, \mathbb{C})$ is generated by derivatives of the differential $y(\xi) dx$ with respect to the modulus ξ . For two-parameter curves the cohomology group $H^1(\Sigma, \mathbb{C})$ still has the same dimension $2g$ and can be generated by $y(\xi, \eta) dx$ and derivatives with respect to ξ , η or combinations of both derivatives. This gives a freedom in writing down quantum differential operators $\hbar^{2n} \mathcal{D}_{2n}$ for multi-moduli curves. We prefer choosing derivatives with respect to the modulus ξ only, since as a second consistency check we can then take the limit $\eta \rightarrow 0$ giving back the old quantum differential operators (4.34). The first operator $\hbar^2 \mathcal{D}_2$ is exemplarily written down in appendix D.

In this new setting of two-parameter curves it would be interesting to analyse how one could recover the WKB periods, in particular, the transcendental numbers or a closed expression for F_1 . A guess could be that transcendental numbers arise from summing up contributions in the new parameter if one restricts to special limits in η . Furthermore, tuning η could transform different quantum mechanical models into each other. For example taking $\eta = \frac{4}{5}$ transforms the quintic anharmonic oscillator potential to a potential of the form $\frac{9}{10}x^2 - \frac{4}{5}x^4 - x^5$ having four extrema, see Fig. 4.8. In the language of the curve this would yield five branch points located on the real axis. Constructing a symplectic basis of cycles on a genus two surface is well understood, for example as shown in Fig. 2.1. In this construction it is not necessary that the branch points lie on the real axis. For the quantum mechanical interpretation it makes a significant difference because these cycles encircle the classically allowed or forbidden regions. Additional allowed or forbidden regions can be interpreted as additional vacua and eventually tunneling contributions have to be taken into account. Perhaps in the WKB framework one has to regard more periods which are not considered so far. With our methods it is feasible to compute such periods but future work is required to give them a proper quantum mechanical interpretation. In this perspective analyzing the transition between anharmonic oscillators and more general potentials of different shapes could perhaps extend the theory of one-dimensional quantum mechanical systems, for instance, to generalized quantization conditions as proposed in [34–36, 40].

Acknowledgements

We would like to thank Hans Jockers and Thorsten Schimannek for useful conversations. Special thanks to Marcos Mariño for sharing his insights into the subject during collaboration in the initial state of the project. We further thank the Bonn-Cologne Graduate School of Physics and Astronomy (BCGS) for financial support. F.F. also thanks the Studienstiftung des deutschen Volkes for support and A. K. thanks the MSRI in Berkeley for hospitality during the final stage of this work.

A Residues of Abelian Differentials on the WKB Curve

This appendix provides auxiliary residue calculations on the WKB curve $\Sigma : y^2 = 2\xi - x^2 + 2x^d, d \geq 3$ (taken to be non-degenerate). All WKB differentials are linear combinations of one-forms

$$\omega_k^m = \frac{x^m}{y^k} dx, \quad m, k \in \mathbb{Z}, \quad (\text{A.1})$$

so tentative residues are located at infinity or branch points. We begin with points at infinity and discuss the case $d = 2g + 2$ even and $d = 2g + 1$ odd separately.

Case d even. If $d = 2g + 2$, there are two points at infinity $\infty^\pm \in \Sigma$, distinguished by the condition $y/x^{g+1} \rightarrow \pm 1$ as $x \rightarrow \infty$. At those points a local parameter is given by $z = 1/x$, so

$$\omega_k^m = (-1) \frac{(\pm 1)^k}{z^{m+2-kd/2}} \left(2 - z^{d-2} + 2\xi z^d\right)^{-k/2} dz. \quad (\text{A.2})$$

The sign ± 1 refers to the point ∞^\pm respectively. To compute the residue one uses the absolutely convergent binomial series (where $|\chi| < 1$ and $\alpha \in \mathbb{C}$)

$$(1 + \chi)^\alpha = \sum_{s=0}^{\infty} \binom{\alpha}{s} \chi^s, \quad \binom{\alpha}{s} = \begin{cases} \frac{\alpha(\alpha-1)(\alpha-2)\cdots(\alpha-(s-1))}{s!}, & \text{if } s > 0 \\ 1, & \text{if } s = 0 \\ 0, & \text{if } s < 0 \end{cases} \quad (\text{A.3})$$

for the case $\chi = \xi z^d - 1/2 z^{d-2}$ and $\alpha = -k/2$. In summary, the necessary condition for non-vanishing residue is

$$m + 1 - kd/2 \in \{0, 2, 4, \dots\} \quad (\text{A.4})$$

and in this case one finds

$$(\pm 1)^k \text{Res}_{\infty^\pm} \omega_k^m = -2^{-\frac{k}{2}} \sum_{s=0}^{\lfloor s_+ \rfloor} \binom{-k/2}{s} \binom{s}{l_s} (-2)^{l_s-s} \xi^{l_s} \quad (\text{A.5})$$

with

$$s_+ := \frac{m + 1 - kd/2}{d - 2} \quad \text{and} \quad l_s := \frac{d - 2}{2}(s_+ - s). \quad (\text{A.6})$$

The necessary condition is only satisfied for $n = 0$, as $k = 3n - 1$ and $m \leq n(d - 1)$ for the WKB differentials.

Case d odd. For odd $d = 2g + 1$ there is only one point at infinity $\infty \in \Sigma$ together with a local parameter $z = 1/\sqrt{x}$. The residue at infinity is given by

$$\text{Res}_\infty \omega_k^m = -2^{1-\frac{k}{2}} \sum_{s=0}^{\lfloor s_+ \rfloor} \binom{-k/2}{s} \binom{s}{l_s} (-2)^{l_s-s} \xi^{l_s} \mathbf{1}_{\mathbb{N}}(l_s) \quad (\text{A.7})$$

with

$$\mathbb{1}_{\mathbb{N}}(l) := \begin{cases} 1, & \text{if } l \in \{0, 1, 2, \dots\} \\ 0, & \text{otherwise.} \end{cases} \quad (\text{A.8})$$

Necessary conditions for a non-zero residue are

$$k \text{ even} \quad \text{and} \quad m + 1 - kd/2 \geq 0. \quad (\text{A.9})$$

For even n the number $k = 3n - 1$ is odd, so \mathcal{Q}_n has zero residue at infinity.

Behavior at branch points. Turning to the behavior of ω_k^m at the d finite branch points where $p^2(x) = 0$, one has as local parameter $z = \sqrt{x - x_j}$. Thus

$$\omega_k^m = \frac{(z^2 + x_j)^m}{\sqrt{\prod_{i \neq j} (z^2 + (x_j - x_i))}^k} \frac{2}{z^{k-1}} dz \quad (\text{A.10})$$

and the first factor is a holomorphic even function of z . Consequently if k is odd, ω_k^m has zero residue at the branch points. Indeed, $k = 3n - 1$ is odd for terms in the WKB differentials \mathcal{Q}_n with even n .

B Evaluation of Period Integrals

We have seen that the Picard-Fuchs equation easily yields expansions for period integrals in terms of their respective parameters up to arbitrarily high order. As the equation can be obtained from the differential and solved with modest effort, the only laborious point is to find the leading terms of the expansions in order to fix the correct linear combination of solutions.²³ Here the classical WKB periods $\oint_{A,B} y \, dx$ are defined by explicit specification of the homology cycle and shall be evaluated in the following. Our approach applies to all hyperelliptic curves of the form

$$y^2 = 2\xi - x^2 + 2x^d \quad \text{with } d > 2. \quad (\text{B.1})$$

For $d > 4$ this is particularly interesting as generically no closed expressions (say in terms of special functions) are known for the hyperelliptic integrals over $y(x, \xi) \, dx$. For the sake of clarity we will focus on the case $d = 5$.

Recall that the A - and B -cycle are defined such that they encircle pairs of branch points as given in Fig. 4.4.²⁴ There are no radical expressions for the branch points, which trace out trajectories in the complex plane as ξ is being varied in an interval I . As the value of the period does not change when replacing the integration contour by a larger one of the same homology class, we can choose a contour sufficiently large to enclose the full trajectories of the respective branch points, hence giving (locally) a ξ -independent integration contour.

Consider $I = [0, v]$ with the root v of Δ . The series we will obtain for the A -period will be convergent in a disc $D_v(0)$, whereas the B -period will be convergent and single-valued in $D_v(0) \setminus [-v, 0)$ due to the branch cut of the logarithm (which we take to lie on $\mathbb{R}_{<0}$). For the quintic we find²⁵

$$\begin{aligned} \nu^{(0)}(\xi) &= \frac{1}{\pi} \int_{x_0}^{\xi^{5-1/3}} \sqrt{2\xi - x^2 + 2x^5} \, dx \\ \nu_D^{(0)}(\xi) &= -2i \int_0^{\xi^{2-1/3}} \sqrt{2\xi - x^2 + 2x^5} \, dx. \end{aligned} \quad (\text{B.2})$$

The computation is based on the ξ -expansion of the integrand

$$y(x, \xi) = \sqrt{2\xi - x^2 + 2x^5} = \sqrt{2x^5 - x^2} + \frac{\xi}{\sqrt{2x^5 - x^2}} - \frac{\xi^2}{\sqrt{2x^5 - x^2}} + \mathcal{O}(\xi^3) \quad (\text{B.3})$$

which however is invalid for roots of $2x^5 - x^2 = 0$ (an appropriate branch choice understood). As such roots lie within the integration range (A -period) or at its boundary (B -period), the range has to be split and a Cauchy principal value prescription to be used. In case of the A -period we obtain

$$\nu^{(0)}(\xi) = \xi + \frac{315}{16} \xi^4 + \mathcal{O}(\xi^7). \quad (\text{B.4})$$

²³As mentioned in section 2.2, monodromy considerations already allow for partial identification of the periods.

²⁴In our convention branch cuts lie between branch points where $(\xi - V(x))$ is negative.

²⁵Here we set $x_0 = \frac{1}{3} \left(\sqrt[3]{2} - \sqrt[3]{\frac{5}{2}} - \frac{2}{\sqrt[3]{5}} \right) < 0$.

For the second integral in (B.2) we split the integration range into three parts

$$\left[0, 2^{-1/3}\right] = \left[0, \epsilon\right] + \left[\epsilon, 2^{-1/3} - \delta\right] + \left[2^{-1/3} - \delta, 2^{-1/3}\right] \quad (\text{B.5})$$

where the middle part gives with the help of (B.3)

$$\begin{aligned} -2i \int_{\epsilon}^{2^{-1/3}-\delta} \sqrt{2\xi - x^2 + 2x^5} \, dx &= \frac{\sqrt{\pi} \Gamma\left(\frac{5}{3}\right)}{2 \cdot 2^{2/3} \Gamma\left(\frac{13}{6}\right)} + 2\xi \log(\epsilon) - \frac{2}{3}\xi \log(2) \\ &\quad - \frac{2\sqrt{\frac{2}{3}}}{3\sqrt{\delta}}\xi^2 - \frac{1}{2\epsilon^2}\xi^2 - \frac{7\pi \Gamma\left(-\frac{1}{3}\right)}{9 \Gamma\left(-\frac{1}{6}\right) \Gamma\left(\frac{5}{6}\right)}\xi^2 + \mathcal{O}(\xi^3). \end{aligned} \quad (\text{B.6})$$

Here we have neglected higher order terms in ϵ and δ as they vanish for $\epsilon, \delta \rightarrow 0$ eventually. For the first integration part we do not use (B.3) as it stands. Here, we first factorize $y^2 = \prod_{i=1}^5 (x - e_i(\xi))$ where the roots e_i can be computed perturbatively in ξ . Since the integration variable x is arbitrarily small for this integration range we expand the square root of three linear factors in x and then perform the integration termwise. These three linear factors are picked by the condition that $e_i \rightarrow 0$ as $\xi \rightarrow 0$. Expanding the intermediate result again in ξ we obtain for the first part

$$-2i \int_0^{\epsilon} \sqrt{2\xi - x^2 + 2x^5} \, dx = -(-\log(\xi) + 2\log(\epsilon) + 1 + \log(2))\xi + \frac{\xi^2}{2\epsilon^2} + \mathcal{O}(\xi^3). \quad (\text{B.7})$$

The same strategy can be applied to the upper integration domain. As it turns out, this part does not give any finite contributions to the final result. It merely cancels singular terms in δ .

Adding all three contributions we finally obtain the leading behaviour of the B -period

$$\begin{aligned} -2i \int_0^{\epsilon} \sqrt{2\xi - x^2 + 2x^5} \, dx \\ = \frac{\sqrt{\pi} \Gamma\left(\frac{5}{3}\right)}{2 \cdot 2^{2/3} \Gamma\left(\frac{13}{6}\right)} - \left(1 - \log\left(\frac{\xi}{2^{5/3}}\right)\right)\xi - \frac{7\pi \Gamma\left(-\frac{1}{3}\right)}{9 \Gamma\left(-\frac{1}{6}\right) \Gamma\left(\frac{5}{6}\right)}\xi^2 + \mathcal{O}(\xi^3). \end{aligned} \quad (\text{B.8})$$

For the higher order WKB periods one could do a similar computation. Fortunately, this is not necessary because the operators \mathcal{D}_{2n} allow us to compute the quantum corrections directly from the classical periods.

C Picard-Fuchs Operators for WKB Periods

In this appendix we collect the Picard-Fuchs operators annihilating the WKB periods for the quintic and sextic anharmonic oscillator. Results include the leading and the first three subleading orders corresponding to WKB periods of order $\{\hbar^0, \hbar^2, \hbar^4, \hbar^6\}$. In the present notation the differential operator $\mathcal{L}_{\text{PF}}^{(2n)}$ annihilates the WKB periods $\nu^{(2n)} \hbar^{2n}$ and $\nu_D^{(2n)} \hbar^{2n}$.

On first sight it seems that in higher order Picard-Fuchs operators new singularities arise in terms of additional zeroes of the polynomial multiplying the highest derivative. However, these are spurious poles since writing the Picard-Fuchs equation in a coordinate centered at such a point one obtains a fundamental system spanned by regular solutions. This is in accordance with our geometric expectation: the radius of convergence of a solution is determined by the distance to the nearest degeneration point, which must be a root of the discriminant. Clearly, the respective discriminant appears in all Picard-Fuchs operators of the sextic and quintic periods.

Picard-Fuchs Operators for the Sextic Oscillator

$$\begin{aligned} \mathcal{L}_{\text{PF}}^{(0)} = & (54\xi^2 - 1) \xi \partial_\xi^4 \\ & + 2(162\xi^2 - 1) \partial_\xi^3 \\ & + 354 \xi \partial_\xi^2 \\ & + 30 \partial_\xi \end{aligned} \tag{C.1}$$

$$\begin{aligned} \mathcal{L}_{\text{PF}}^{(2)} = & (54\xi^2 - 1)(1782\xi^2 - 65) \xi^1 \partial_\xi^3 \\ & + 3(224532\xi^4 - 11124\xi^2 + 65) \partial_\xi^2 \\ & + 66(14418\xi^2 - 947) \xi \partial_\xi \\ & + 96(1782\xi^2 - 185) \end{aligned} \tag{C.2}$$

$$\begin{aligned} \mathcal{L}_{\text{PF}}^{(4)} = & \xi(54\xi^2 - 1)(7409920500\xi^4 - 330245820\xi^2 + 9632693) \partial_\xi^3 \\ & + 5(880298555400\xi^6 - 47848497228\xi^4 + 1758643758\xi^2 - 9632693) \partial_\xi^2 \\ & + 30\xi(398653722900\xi^4 - 24604325820\xi^2 + 1016813357) \partial_\xi \\ & + 960(7409920500\xi^4 - 486072540\xi^2 + 40410853) \end{aligned} \tag{C.3}$$

$$\begin{aligned} \mathcal{L}_{\text{PF}}^{(6)} = & \xi(54\xi^2 - 1)(1593291078484200\xi^6 + 86962831950060\xi^4 + 7919960534814\xi^2 - 50291624911) \partial_\xi^3 \\ & + (1290565773572202000\xi^8 + 78238588651670880\xi^6 + 7864991012868984\xi^4 \\ & \quad - 96630505323144\xi^2 + 352041374377) \partial_\xi^2 \\ & + (\xi 868343637773889000\xi^6 + 63008309812806540\xi^4 + 7170473076071550\xi^2 \\ & \quad - 50170087365031) \partial_\xi \\ & + 30240(177032342053800\xi^6 + 16620344819244\xi^4 + 1987953607118\xi^2 - 28451410671) \end{aligned} \tag{C.4}$$

Picard-Fuchs Operators for the Quintic Oscillator

$$\begin{aligned}
\mathcal{L}_{\text{PF}}^{(0)} = & (25000\xi^3 - 27) \xi \partial_\xi^4 \\
& + (200000\xi^3 - 54) \partial_\xi^3 \\
& + 317500 \xi^2 \partial_\xi^2 \\
& + 35000 \xi \partial_\xi \\
& + \frac{6545}{2}
\end{aligned} \tag{C.5}$$

$$\begin{aligned}
\mathcal{L}_{\text{PF}}^{(2)} = & 2 (32000000\xi^3 + 193347) (25000\xi^3 - 27) \xi \partial_\xi^4 \\
& + 8 (26000000000000\xi^6 + 19118700000\xi^3 - 5220369) \partial_\xi^3 \\
& + 125000 (573440000\xi^3 + 5525577) \xi^2 \partial_\xi^2 \\
& + 18000 (3656000000\xi^3 + 49908357) \xi \partial_\xi \\
& + 267995 (32000000\xi^3 + 720657)
\end{aligned} \tag{C.6}$$

$$\begin{aligned}
\mathcal{L}_{\text{PF}}^{(4)} = & 2\xi (25000\xi^3 - 27) (33013760000000000\xi^6 + 1565984563200000\xi^3 + 6305572607481) \partial_\xi^4 \\
& + 36 (8253440000000000000000\xi^9 + 45674549760000000000\xi^6 + 203138823048300000\xi^3 \\
& - 56750153467329) \partial_\xi^3 \\
& + 5000 (31726223360000000000\xi^6 + 2051693233459200000\xi^3 + 11526405450672231) \xi^2 \partial_\xi^2 \\
& + 14000 (198907904000000000000\xi^6 + 1504793310105600000\xi^3 + 11080573290031581) \xi \partial_\xi \\
& + 1216215 (990412800000000000\xi^6 + 8399258009600000\xi^3 + 109484562862143)
\end{aligned} \tag{C.7}$$

$$\begin{aligned}
\mathcal{L}_{\text{PF}}^{(6)} = & 2\xi (25000\xi^3 - 27) (108190984437760000000000\xi^6 - 2201331444040108800000\xi^3 \\
& - 1084714198114610277) \partial_\xi^4 \\
& + 16 (8790517485568000000000000000\xi^9 - 2002259512610897400000000000\xi^6 \\
& - 71323951693284191700000\xi^3 + 29287283349094477479) \partial_\xi^3 \\
& + 35000 (334001024814284800000000000\xi^6 - 849330559112858956800000\xi^3 \\
& - 561279483265056745473) \xi^2 \partial_\xi^2 \\
& + 14000 (2554466421850112000000000000\xi^6 - 7321188595679726472000000\xi^3 \\
& - 5333494905100446357357) \xi \partial_\xi \\
& + 210900515 (154558549196800000000000\xi^6 - 502837975009094400000\xi^3 - 627242552904521151)
\end{aligned} \tag{C.8}$$

D Differential Operators for Quantum Corrections

As for the one-parameter models we compute differential operators which applied on the classical periods give the quantum corrections at a certain order in \hbar . In the two-parameter models these operators get quite messy. An example is given for $\hbar^2 \mathcal{D}_2$

$$\begin{aligned}
\mathcal{D}_2 = & \left[(8\eta^3 - 25\eta - 25) \xi \left(800000\eta (4\eta^3 - 15\eta - 15) \xi^4 - (-8\eta^3 + 27\eta + 27)^2 (\eta + 1)^6 - 64\eta^2 (768\eta^6 - 5584\eta^4 \right. \right. \\
& - 5584\eta^3 + 10125\eta^2 + 20250\eta + 10125) (\eta + 1)^2 \xi^2 + 12\eta (256\eta^6 - 1784\eta^4 - 1784\eta^3 \\
& + 3105\eta^2 + 6210\eta + 3105) (\eta + 1)^4 \xi + 8 (32768\eta^9 - 250880\eta^7 - 250880\eta^6 + 455000\eta^5 + 910000\eta^4 \\
& + 539375\eta^3 + 253125\eta^2 + 253125\eta + 84375) \xi^3 \left. \right)] / \\
& [-3072\eta^{14} + 3072\eta^{13}(32\xi - 5) - 192\eta^{12}(4096\xi^2 - 1536\xi + 17) - 384\eta^{11}(2048\xi^2 + 1592\xi - 349) \\
& + 96\eta^{10}(74880\xi^2 - 36736\xi + 3293) + 96\eta^9(14336\xi^3 + 149760\xi^2 - 28044\xi - 171) + 3\eta^8(-4797440\xi^2 \\
& + 3367040\xi - 399669) - 24\eta^7(384000\xi^3 + 2697600\xi^2 - 992680\xi + 84801) - 12\eta^6(768000\xi^3 \\
& + 3631200\xi^2 - 926880\xi + 53467) + 24\eta^5(640000\xi^3 + 2628800\xi^2 - 1129080\xi + 108297) \\
& + 6\eta^4(5120000\xi^3 + 21168000\xi^2 - 8614464\xi + 799281) + 24\eta^3(640000\xi^3 + 3528000\xi^2 - 1701000\xi \\
& + 175257) + 3780\eta^2(5600\xi^2 - 4320\xi + 567) - 68040\eta(40\xi - 9) + 76545] \cdot \partial_\xi^3 \\
+ & \left[-3(-8\eta^3 + 27\eta + 27)^2 (16\eta^3 - 55\eta - 55) (\eta + 1)^6 + 128000\eta (3712\eta^6 - 25400\eta^4 - 25400\eta^3 \right. \\
& + 43125\eta^2 + 86250\eta + 43125) \xi^4 - 32\eta^2 (106496\eta^9 - 1155840\eta^7 - 1155840\eta^6 + 4149160\eta^5 + 8298320\eta^4 \\
& - 781715\eta^3 - 14792625\eta^2 - 14792625\eta - 4930875) (\eta + 1)^2 \xi^2 + 8\eta (22528\eta^9 - 235520\eta^7 - 235520\eta^6 \\
& + 818472\eta^5 + 1636944\eta^4 - 127203\eta^3 - 2837025\eta^2 - 2837025\eta - 945675) (\eta + 1)^4 \xi + 32 (655360\eta^{12} \\
& - 7360512\eta^{10} - 7360512\eta^9 + 25942400\eta^8 + 51884800\eta^7 + 1192400\eta^6 - 74250000\eta^5 - 88171875\eta^4 \\
& - 80437500\eta^3 - 83531250\eta^2 - 55687500\eta - 13921875) \xi^3 \left. \right)] / \\
& [-24576\eta^{14} + 24576\eta^{13}(32\xi - 5) - 1536\eta^{12}(4096\xi^2 - 1536\xi + 17) - 3072\eta^{11}(2048\xi^2 + 1592\xi - 349) \\
& + 768\eta^{10}(74880\xi^2 - 36736\xi + 3293) + 768\eta^9(14336\xi^3 + 149760\xi^2 - 28044\xi - 171) + 24\eta^8(-4797440\xi^2 \\
& + 3367040\xi - 399669) - 192\eta^7(384000\xi^3 + 2697600\xi^2 - 992680\xi + 84801) - 96\eta^6(768000\xi^3 \\
& + 3631200\xi^2 - 926880\xi + 53467) + 192\eta^5(640000\xi^3 + 2628800\xi^2 - 1129080\xi + 108297) \\
& + 48\eta^4(5120000\xi^3 + 21168000\xi^2 - 8614464\xi + 799281) + 192\eta^3(640000\xi^3 + 3528000\xi^2 - 1701000\xi \\
& + 175257) + 30240\eta^2(5600\xi^2 - 4320\xi + 567) - 544320\eta(40\xi - 9) + 612360] \cdot \partial_\xi^2 \\
+ & \left[5(-3\eta(-8\eta^3 + 27\eta + 27))^2 (\eta + 1)^5 + 640\eta (1568\eta^6 - 10700\eta^4 - 10700\eta^3 + 18125\eta^2 + 36250\eta \right. \\
& + 18125) \xi^3 + 48\eta^2 (128\eta^6 - 872\eta^4 - 872\eta^3 + 1485\eta^2 + 2970\eta + 1485) (\eta + 1)^3 \xi - 12 (4096\eta^{10} + 4096\eta^9 \\
& - 19520\eta^8 - 39040\eta^7 - 27520\eta^6 - 24000\eta^5 + 67875\eta^4 + 359500\eta^3 + 551250\eta^2 + 367500\eta + 91875) \xi^2 \left. \right)] / \\
& [-2048\eta^{14} + 2048\eta^{13}(32\xi - 5) - 128\eta^{12}(4096\xi^2 - 1536\xi + 17) - 256\eta^{11}(2048\xi^2 + 1592\xi - 349) \\
& + 64\eta^{10}(74880\xi^2 - 36736\xi + 3293) + 64\eta^9(14336\xi^3 + 149760\xi^2 - 28044\xi - 171) + 2\eta^8(-4797440\xi^2 \\
& + 3367040\xi - 399669) - 16\eta^7(384000\xi^3 + 2697600\xi^2 - 992680\xi + 84801) - 8\eta^6(768000\xi^3 + 3631200\xi^2 \\
& - 926880\xi + 53467) + 16\eta^5(640000\xi^3 + 2628800\xi^2 - 1129080\xi + 108297) + 4\eta^4(5120000\xi^3 \\
& + 21168000\xi^2 - 8614464\xi + 799281) + 16\eta^3(640000\xi^3 + 3528000\xi^2 - 1701000\xi + 175257) \\
& + 2520\eta^2(5600\xi^2 - 4320\xi + 567) - 45360\eta(40\xi - 9) + 51030] \cdot \partial_\xi
\end{aligned} \tag{D.1}$$

$$\begin{aligned}
& + \left[35 \left(32\eta (-8\eta^3 + 25\eta + 25)^2 \xi^2 + 3\eta^2 (8\eta^3 - 27\eta - 27) (\eta + 1)^4 - 3 (512\eta^6 - 2960\eta^4 - 2960\eta^3 \right. \right. \\
& \quad \left. \left. + 4125\eta^2 + 8250\eta + 4125) (\eta + 1)^2 \xi \right) \right] / \\
& \left[-1024\eta^{14} + 1024\eta^{13}(32\xi - 5) - 64\eta^{12} (4096\xi^2 - 1536\xi + 17) - 128\eta^{11} (2048\xi^2 + 1592\xi - 349) \right. \\
& \quad + 32\eta^{10} (74880\xi^2 - 36736\xi + 3293) + 32\eta^9 (14336\xi^3 + 149760\xi^2 - 28044\xi - 171) + \eta^8 (-4797440\xi^2 \\
& \quad + 3367040\xi - 399669) - 8\eta^7 (384000\xi^3 + 2697600\xi^2 - 992680\xi + 84801) - 4\eta^6 (768000\xi^3 + 3631200\xi^2 \\
& \quad - 926880\xi + 53467) + 8\eta^5 (640000\xi^3 + 2628800\xi^2 - 1129080\xi + 108297) + 2\eta^4 (5120000\xi^3 + 21168000\xi^2 \\
& \quad - 8614464\xi + 799281) + 8\eta^3 (640000\xi^3 + 3528000\xi^2 - 1701000\xi + 175257) + 1260\eta^2 (5600\xi^2 - 4320\xi \\
& \quad \left. + 567) - 22680\eta(40\xi - 9) + 25515 \right] .
\end{aligned}$$

References

- [1] N. Seiberg and E. Witten, “Electric - magnetic duality, monopole condensation, and confinement in $N=2$ supersymmetric Yang-Mills theory,” *Nucl. Phys.* **B426** (1994) 19–52, [arXiv:hep-th/9407087 \[hep-th\]](#). [Erratum: *Nucl. Phys.* B430,485(1994)].
- [2] A. Klemm, W. Lerche, and S. Theisen, “Nonperturbative effective actions of $N=2$ supersymmetric gauge theories,” *Int. J. Mod. Phys.* **A11** (1996) 1929–1974, [arXiv:hep-th/9505150 \[hep-th\]](#).
- [3] S. H. Katz, A. Klemm, and C. Vafa, “Geometric engineering of quantum field theories,” *Nucl. Phys.* **B497** (1997) 173–195, [arXiv:hep-th/9609239 \[hep-th\]](#).
- [4] T. M. Chiang, A. Klemm, S.-T. Yau, and E. Zaslow, “Local mirror symmetry: Calculations and interpretations,” *Adv. Theor. Math. Phys.* **3** (1999) 495–565, [arXiv:hep-th/9903053 \[hep-th\]](#).
- [5] G. Akemann, “Higher genus correlators for the Hermitian matrix model with multiple cuts,” *Nucl. Phys.* **B482** (1996) 403–430, [arXiv:hep-th/9606004 \[hep-th\]](#).
- [6] N. A. Nekrasov and S. L. Shatashvili, “Quantization of Integrable Systems and Four Dimensional Gauge Theories,” in *Proceedings, 16th International Congress on Mathematical Physics (ICMP09): Prague, Czech Republic, August 3-8, 2009*, pp. 265–289. 2009. [arXiv:0908.4052 \[hep-th\]](#).
- [7] M. Aganagic, R. Dijkgraaf, A. Klemm, M. Marino, and C. Vafa, “Topological strings and integrable hierarchies,” *Commun. Math. Phys.* **261** (2006) 451–516, [arXiv:hep-th/0312085 \[hep-th\]](#).
- [8] L. F. Alday, D. Gaiotto, and Y. Tachikawa, “Liouville Correlation Functions from Four-dimensional Gauge Theories,” *Lett. Math. Phys.* **91** (2010) 167–197, [arXiv:0906.3219 \[hep-th\]](#).
- [9] S. Bloch, M. Kerr, and P. Vanhove, “Local mirror symmetry and the sunset Feynman integral,” [arXiv:1601.08181 \[hep-th\]](#).
- [10] N. A. Nekrasov, “Seiberg-Witten prepotential from instanton counting,” *Adv. Theor. Math. Phys.* **7** no. 5, (2003) 831–864, [arXiv:hep-th/0206161 \[hep-th\]](#).
- [11] J. Choi, S. Katz, and A. Klemm, “The refined BPS index from stable pair invariants,” *Commun. Math. Phys.* **328** (2014) 903–954, [arXiv:1210.4403 \[hep-th\]](#).
- [12] A. Brini, M. Marino, and S. Stevan, “The Uses of the refined matrix model recursion,” *J. Math. Phys.* **52** (2011) 052305, [arXiv:1010.1210 \[hep-th\]](#).

- [13] V. Bouchard, A. Klemm, M. Marino, and S. Pasquetti, “Remodeling the B-model,” *Commun. Math. Phys.* **287** (2009) 117–178, [arXiv:0709.1453 \[hep-th\]](#).
- [14] M. Aganagic, M. C. N. Cheng, R. Dijkgraaf, D. Krefl, and C. Vafa, “Quantum Geometry of Refined Topological Strings,” *JHEP* **11** (2012) 019, [arXiv:1105.0630 \[hep-th\]](#).
- [15] S. Codesido and M. Marino, “Holomorphic Anomaly and Quantum Mechanics,” *J. Phys.* **A51** no. 5, (2018) 055402, [arXiv:1612.07687 \[hep-th\]](#).
- [16] A. Grassi and J. Gu, “Argyres-Douglas theories, Painlevé II and quantum mechanics,” [arXiv:1803.02320 \[hep-th\]](#).
- [17] M. Bershadsky, S. Cecotti, H. Ooguri, and C. Vafa, “Kodaira-Spencer theory of gravity and exact results for quantum string amplitudes,” *Commun. Math. Phys.* **165** (1994) 311–428, [arXiv:hep-th/9309140 \[hep-th\]](#).
- [18] M.-x. Huang and A. Klemm, “Direct integration for general Ω backgrounds,” *Adv. Theor. Math. Phys.* **16** no. 3, (2012) 805–849, [arXiv:1009.1126 \[hep-th\]](#).
- [19] D. Krefl and J. Walcher, “Extended Holomorphic Anomaly in Gauge Theory,” *Lett. Math. Phys.* **95** (2011) 67–88, [arXiv:1007.0263 \[hep-th\]](#).
- [20] M.-x. Huang and A. Klemm, “Holomorphic Anomaly in Gauge Theories and Matrix Models,” *JHEP* **09** (2007) 054, [arXiv:hep-th/0605195 \[hep-th\]](#).
- [21] B. Haghighat, A. Klemm, and M. Rauch, “Integrability of the holomorphic anomaly equations,” *JHEP* **10** (2008) 097, [arXiv:0809.1674 \[hep-th\]](#).
- [22] M.-x. Huang, A.-K. Kashani-Poor, and A. Klemm, “The Ω deformed B-model for rigid $\mathcal{N} = 2$ theories,” *Annales Henri Poincaré* **14** (2013) 425–497, [arXiv:1109.5728 \[hep-th\]](#).
- [23] M.-x. Huang, “On Gauge Theory and Topological String in Nekrasov-Shatashvili Limit,” *JHEP* **06** (2012) 152, [arXiv:1205.3652 \[hep-th\]](#).
- [24] M.-x. Huang, A. Klemm, J. Reuter, and M. Schiereck, “Quantum geometry of del Pezzo surfaces in the Nekrasov-Shatashvili limit,” *JHEP* **02** (2015) 031, [arXiv:1401.4723 \[hep-th\]](#).
- [25] A. Klemm, M. Poretschkin, T. Schimannek, and M. Westerholt-Raum, “Direct Integration for Mirror Curves of Genus Two and an Almost Meromorphic Siegel Modular Form,” [arXiv:1502.00557 \[hep-th\]](#).

- [26] T. Gulden, M. Janas, P. Koroteev, and A. Kamenev, “Statistical mechanics of Coulomb gases as quantum theory on Riemann surfaces,” *Zh. Eksp. Teor. Fiz.* **144** (2013) 574, [arXiv:1303.6386](#) [cond-mat.stat-mech]. [*J. Exp. Theor. Phys.*117,517(2013)].
- [27] M. Kreshchuk and T. Gulden, “The Picard-Fuchs equation in classical and quantum physics: Application to higher-order WKB method,” [arXiv:1803.07566](#) [hep-th].
- [28] J. L. Dunham, “The wenzel-brillouin-kramers method of solving the wave equation,” *Phys. Rev.* **41** (Sep, 1932) 713–720.
- [29] A. Galindo and P. Pascual, *Quantum Mechanics II*. Texts and Monographs in Physics. Springer-Verlag, 1991.
- [30] S. Donaldson, *Riemann Surfaces*. Oxford Graduate Texts in Mathematics. Oxford University Press, 2011.
- [31] E. Ince, *Ordinary Differential Equations*. Dover Books on Mathematics. Dover Publications, 1956.
- [32] C. Bender and S. Orszag, *Advanced Mathematical Methods for Scientists and Engineers I: Asymptotic Methods and Perturbation Theory*. Springer-Verlag, 1978.
- [33] P. Candelas, X. C. De La Ossa, P. S. Green, and L. Parkes, “A Pair of Calabi-Yau manifolds as an exactly soluble superconformal theory,” *Nucl. Phys.* **B359** (1991) 21–74. [*AMS/IP Stud. Adv. Math.*9,31(1998)].
- [34] J. Zinn-Justin and U. D. Jentschura, “Multi-instantons and exact results I: Conjectures, WKB expansions, and instanton interactions,” *Annals Phys.* **313** (2004) 197–267, [arXiv:quant-ph/0501136](#) [quant-ph].
- [35] J. Zinn-Justin and U. D. Jentschura, “Multi-instantons and exact results II: Specific cases, higher-order effects, and numerical calculations,” *Annals Phys.* **313** (2004) 269–325, [arXiv:quant-ph/0501137](#) [quant-ph].
- [36] U. D. Jentschura, A. Surzhykov, and J. Zinn-Justin, “Multi-instantons and exact results. III: Unification of even and odd anharmonic oscillators,” *Annals Phys.* **325** (2010) 1135–1172.
- [37] I. Gahramanov and K. Tezgin, “Remark on the Dunne-Ünsal relation in exact semiclassics,” *Phys. Rev.* **D93** no. 6, (2016) 065037, [arXiv:1512.08466](#) [hep-th].
- [38] G. Álvarez and C. Casares, “Uniform asymptotic and jwkb expansions for anharmonic oscillators,” *J. Phys. A* **33** no. 13, (2000) 2499.

- [39] A. Bobenko and C. Klein, *Computational Approach to Riemann Surfaces*. No. Nr. 2013 in Lecture Notes in Mathematics. Springer-Verlag, 2011.
- [40] E. Delabaere, H. Dillinger, and F. Pham, “Exact semiclassical expansions for one-dimensional quantum oscillators,” *J. Math. Phys.* **38** no. 12, (1997) 6126–6184, <http://dx.doi.org/10.1063/1.532206>.